Madan Bhandari College of Engineering

Faculty of Science and Technology

Madan Bhandari Memorial Academy

Joint Constituent College of Pokhara University (PoU),

Urlabari - 03, Morang, Nepal

A

Final Year Project Report on

" Soil Loss and Erosion Susceptibility Prediction using USLE and RUSLE Models: Evidence from Miklajung Siwalik Hills, Nepal Himalaya"

Submitted to the department of civil engineering in partial fulfillment of the requirements for the degree of bachelor's in civil engineering

(Subject code: CVL- 490)

SUPERVISOR

Er. Chakra Bhandari

(Lecturer, Madan Bhandari College of Engineering)

SUBMITTED BY

Aakrit Dhakal (077/BCE/01)

Anish Lawati (077/BCE/04)

Arpan Karki (077/BCE/10)

Bimosh Basnet (077/BCE/20)

Himal Bhandari (077/BCE/31)

Jarman Rai (077/BCE/33)

September 2025

DEDICATION

This work is lovingly dedicated to the farmers and communities whose livelihoods depend on the soil, and to all those who strive to protect our land from degradation.

Copyright ©

Declaration of Authorship

The Project entitled " Soil Loss and Erosion Susceptibility Prediction using USLE and RUSLE Models: Evidence From Miklajung Siwalik Hills, Nepal Himalaya" ,which is being submitted to the Department of Civil Engineering, Madan Bhandari College of Engineering, Urlabari-03, Morang, Nepal; for the award of the degree of Bachelor in Civil Engineering is a Project work Carried out by us under the Supervision of Er. Chakra Bhandari (Lecturer, Madan Bhandari College of Engineering, PoU). We declare that this project work is entirely our own, and it has not been previously submitted by us or anyone else at any university for any academic recognition or award.

Moreover, we affirm that proper acknowledgment has been given to materials sourced from other references in the thesis. We accept sole responsibility for any instances of irregularities and illegal activities that may be identified in the Project.

Project Members:

Aakrit Dhakal (077/BCE/01)

Anish Lawati (077/BCE/04)

Arpan Karki (077/BCE/10)

Bimosh Basnet (077/BCE/20)

Himal Bhandari (077/BCE/31)

Jarman Rai (077/BCE/33)

Madan Bhandari College of Engineering

Faculty of Science and Technology

Madan Bhandari Memorial Academy

Joint Constituent College of Pokhara University (PoU),

Urlabari - 03, Morang, Nepal

Certificate of Approval

This is to certify that this project work entitled **" Soil Loss and Erosion Susceptibility Prediction using USLE and RUSLE Models: Evidence from Miklajung Siwalik Hills, Nepal Himalaya"** has been examined and has been declared successful for the fulfillment of the academic requirements towards the completion of the bachelor's degree in civil engineering.

.....	.....	.....
Er. Chakra Bhandari	**Er. Ribash Dahal**	**Er. Anubhav Pokhrel**
Supervisor	Internal Examiner	External Examiner

.....

Assistant Professor, Paribesh Timsina

Head of Department (HoD)

Madan Bhandari College of Engineering, Urlabari-03, Nepal

This page is left intentionally blank…

Abstract

Soil erosion is a critical environmental challenge in mountainous regions such as Nepal, where fragile landscapes and intensive land use exacerbate land degradation. This study assesses soil loss in the Bakraha Watershed by applying the Universal Soil Loss Equation (USLE) and the Revised Universal Soil Loss Equation (RUSLE) within a GIS and remote sensing framework. Twenty stations' daily rainfall records spanning 24 years were analyzed to develop the rainfall erosivity (R) factor, while soil erodibility (K) was derived from NARC organic content maps and laboratory analyses. Topographic factors (L and S) were generated from DEM derivatives in ArcGIS, and land cover management factors (C and P) were quantified using LULC classification and NDVI from Google Earth Engine. The results revealed soil erosion rates ranging from 0 to 515 t ha^{-1} yr^{-1} (mean: 10.51 t ha^{-1} yr^{-1}) under USLE and 0 to 5852.88 t ha^{-1} yr^{-1} (mean: 16.65 t ha^{-1} yr^{-1}) under RUSLE. High erosion susceptibility was concentrated in barren lands, steep slopes (>26.8%), and agricultural areas, while forests and grasslands experienced comparatively lower rates. Validation through AU-ROC analysis confirmed strong predictive capability, with RUSLE outperforming USLE in capturing spatial heterogeneity. These findings highlight the severe erosion risk in the Bakraha watershed and underscore the value of integrating RUSLE with GIS and remote sensing for watershed-scale erosion assessment, providing a scientific basis for sustainable land management and conservation planning in data-scarce Himalayan environments.

Keywords: Revised Universal Soil Loss, Digital Elevation Model, Geospatial modeling, Geographical Information System.

Acknowledgement

This project report on **"Soil Loss and Erosion Susceptibility Prediction using USLE and RUSLE Models: Evidence from Miklajung Siwalik Hills, Nepal Himalaya"** ,is prepared with a collective effort of the project members, Project Supervisor, Department of Civil Engineering of Madan Bhandari College of Engineering, Lecturers and other co-operative fellows. We are highly indebted to Er. Chakra Bhandari, Madan Bhandari College of Engineering, for his wise and patient guidance, encouragement and assistance throughout the project work. His dedicated guidance and careful suggestions have accompanied us throughout this journey, challenging us to evolve as engineers and as an individual. His encouragement has spurred us to explore new horizons, unearth my latent talents, and widen our knowledge.

We truly appreciate the support from Asst. Prof. Paribesh Timsina, the Head of Department of Civil Engineering and Prof. Binod Aryal, the Executive Director of Madan Bhandari college of Engineering Urlabari-03, Morang, Nepal for their support and professional response to us. Finally, we would like to express deep gratitude and thanks to our family and friends who were directly and indirectly involved in successful completion of this project.

With heartfelt appreciation

Project members:

Aakrit Dhakal (077/BCE/01)

Anish Lawati (077/BCE/04)

Arpan Karki (077/BCE/10)

Bimosh Basnet (077/BCE/20)

Himal Bhandari (077/BCE/31)

Jarman Rai (077/BCE/33)

List of Figures

List of Tables

List of symbols and Acronyms

AUC	: Area under the Curve
DEM	: Digital Elevation Model
DHM	: Department of Hydrology and Meteorology, Nepal
EUROSEM	: European Soil Erosion Model
GIS	: Geographic Information System
LULC	: Land use and Land cover
MBT	: Main Boundary Thrust
MFT	: Main Frontal Thrust
NDVI	: Normalized Difference Vegetative Index
RUSLE	: Revised Universal Soil Loss Equation
UAV	: Unmanned Aerial Vehicle
USLE	: Universal Soil Loss Equation
WEPP	: Water Erosion Prediction Project

Table of Contents

This page is left intentionally blank…

Chapter 1: Introduction

1.1 Background

Soil is a panacea for all sorts of living things found on the earth. Humans directly utilize more than 70% of the global, ice-free land surface (Rivera et al., 2017) and the anthropogenic pressures on the land and water systems are exacerbating and being stretched to their limits of productivity (FAO, 2021). Soil erosion is one of the gravest environmental threats to the mountainous ecosystems of Nepal causing soil degradation, loss of water quality, and aggravated crop productivity (Chalise et al., 2019). (Chalise et al., 2019) estimated a mean annual soil erosion rate of 11.17 t/ha/yr in the Aringale Khola watershed of Nepal resulting in serious ramifications on soil function and services,(Ghimire et al., 2013a) estimated that 64 t/ha/ yr of sediments is eroded within the Khajuri watershed of Siwalik Hills in Nepal. Rivers in Nepal transport nearly 336 million tons of soil and sediments down to India every year; posing a threat to regional soil and water quality (Tiruwa et al., 2021a)

Soil erosion affects global agricultural production and its long-term sustainability. The impacts of soil erosion vary with soil structure, vegetation cover, and land topography (Lal, 2006)(Pimentel, 2006). Soils with medium to fine texture, low organic matter, and poor structure have higher erosion rates due to low infiltration, reduced aggregate stability, and higher runoff and interflow. Effects may manifold through soil slaking, compaction, and crusting. Soil with limited contact cover, marginal areas, and steep lands are subjected to greater raindrop impact and shearing by wind and water (Pimentel, 2006). Soil erosion results in preferential loss of nutrients, soil organic matter, water availability, and soil thickness, thereby reducing soil quality, biodiversity, and agricultural productivity (Pimentel, 2006; Webster, 2005)

Soil erosion - a process involving the detachment, transport, and deposition of soil particles by water, wind, or gravity, is a global environmental challenge with profound ecological and socioeconomic consequences (Ghimire et al., 2013b). In South Asia, land degradation driven by erosion costs the region an estimated US$10 billion annually, equivalent to 2% of its GDP and 7% of agricultural productivity (Mandal & Kumari, 2020). Nepal, a nation dominated by

tectonically active, mountainous terrain, faces acute erosion risks, particularly in the Siwalik (Churey) Hills, a fragile sedimentary belt forming the foothills of the Himalayas. Here, dynamic geologic processes, including the Indian Plate's ongoing subduction beneath Eurasia (uplifting at ~2 cm/year) (Okamura et al., 2015), steep slopes, loose sedimentary substrates (sandstone, shale, conglomerates), and climate change-amplified monsoonal rainfall converge to create one of Earth's most erosion-prone landscapes (Bastola et al., 2019; McAdoo et al., 2018).

The soil erosion vulnerability in Siwalik zone is exacerbated by anthropogenic pressures, including deforestation, overgrazing, and unsustainable agriculture, which strip protective vegetation and accelerate runoff during intense monsoon rains (June–September) (Dahal, 2020). This interplay of natural and human factors manifests as severe bench, gully, and stream bank erosion, threatening agricultural productivity, hydropower infrastructure, and biodiversity. Despite its ecological and economic significance, soil loss prediction in this region has relied on empirical models like the Universal Soil Loss Equation (USLE) and Revised Universal Soil Loss Equation (RUSLE), which multiplies factors for rainfall erosivity (R), soil erodibility (K), slope length/steepness (LS), cover management (C), and support practices (P) (Siwakoti, 2000).

Recent advances in geospatial technologies offer transformative potential to address these limitations. High-resolution remote sensing (RS), digital terrain models (DTMs), and climate datasets now enable spatially explicit, dynamic modeling of erosion at unprecedented scales (Bhandari et al., 2015).

By leveraging satellite-derived datasets, field surveys, and community input, the model will dynamically adjust RUSLE & USLE factors to reflect real-world erosion drivers, offering high-resolution, spatially explicit risk maps. These outputs will inform targeted soil conservation strategies such as agroforestry, terracing, and riparian buffer zones while advancing scientific understanding of sediment flux in tectonically active landscapes. The proposed study aligns with Nepal's national priorities for climate resilience and sustainable land management. The study aims to formulate a geospatial model using USLE and RUSLE equations combined with GIS for the prediction of soil erosion and sediment yield in the Siwalik Hills of Miklajung.

1.2 Statement of Problem

Soil erosion is critical issue in the Siwalik range of Nepal. The amount of soil loss in the region is very high compared to the other region of Nepal (Tiruwa et al., 2021b). The soil composition is responsible for the soil loss in the region along with the high annual rainfall and steep slope. The extensive anthropogenic factor plays important role in the degradation and erosion of the soil.

The Siwalik range of Nepal, a geologically young and fragile mountain system, faces a severe and widespread problem of soil loss and land degradation. This issue is driven by a combination of natural and human-induced factors, with significant environmental and socioeconomic consequences. The high rate of soil erosion threatens agricultural productivity(Webster, 2005), increases the risk of natural disasters like landslides and floods, and leads to the siltation of vital infrastructure. Soil erosion in the Miklajung Siwalik Zone of Nepal represents a critical environmental and socioeconomic challenge, exacerbated by the region's unique geomorphic fragility, intensifying monsoonal rainfall, and unsustainable land-use practices. Despite decades of research, existing erosion prediction models remain inadequate for guiding effective conservation strategies in this dynamic landscape.

Existing soil erosion assessments in Nepal's Siwalik Hills overwhelmingly rely freely available coarse resolution datasets like DEM and lacks finer spatial analysis along with field validation-neglecting localized variations in soil properties, slope steepness, and land cover(Khanal et al., 2021). Moreover, previous studies include some spatial/technical gaps like Coarse soil/landcover/topography data (>30m resolution) miss micro-erosion hotspots; UAV DEMs underused; models neglect climate links; rainfall projections; lack of R-factor integration. This research is expected to overcome the following problem of statement:

- **Severe Erosion Threat**: Miklajung Siwalik Zone faces critical erosion due to fragile terrain, heavy monsoons, and poor land use.
- **Model Limitations**: Existing models use coarse (>30m) data and lack field validation, missing fine-scale erosion patterns
- **Technical Gaps**: Studies ignore UAV data, R-factor, and socio-economic or climate linkages reducing model accuracy.

This study will Calibrate USLE, RUSLE factors using UAV-derived DEMs to enhance LS-factor accuracy in complex terrain and addresses these gaps through a field-based study and Drone Survey based finer resolution DEM data. Moreover, the model will be validated with field data and sediment yields.

1.3 Aim and Objectives

This project aims to predict and develop a parsimonious soil erosion hotspot model in Miklajung, Tandi Siwalik zone of Nepal Himalaya by integrating USLE and RUSLE equation with GIS in a data-limited environment. The approach involves the detail analysis of the site using the tools like ArcGIS ,field visit for the sample collection combined with the lab testing of the sample testing .The approach involve overcoming some spatial/technical gap like Coarse soil/landcover/topography data (>30m resolution) miss micro-erosion hotspots; UAV DEMs underused; models neglect climate links; rainfall projections; lack of R-factor integration. The following are the secondary objectives to achieve the main objective.

- To develop an integrated geospatial model combining the USLE, RUSLE equations with GIS.
- To predict the soil erosion rate and develop erosion hotspot susceptibility map and validate the result with sediment yield and field data.
- To identify the main environmental and anthropogenic factors that influence soil erosion most strongly in the Miklajung Siwalik zone.

The following Questions will be addressed in this Study:

- How can the USLE and RUSLE equations be effectively integrated with GIS to develop a geospatial soil erosion prediction model?
- What is the spatial distribution of soil erosion risk in the Miklajung Siwalik zone?
- What are the main environmental and anthropogenic factors that influence soil erosion most strongly in the Miklajung Siwalik zone?

These objectives and questions are academically interesting, adequate, and achievable, aligning with the significant impacts of soil erosion and the need for effective disaster risk management strategies in Nepal Himalaya.

Table 1.1:Logical Thinking-Coordination Schema

SN.	Problem statements	Objectives	Research Questions
1	The existing soil erosion prediction models, such as the Universal Soil Loss Equation (USLE) and its revised version, the Revised Universal Soil Loss Equation (RUSLE), are widely used but often fail to account for the highly localized and dynamic erosive forces of concentrated flow, particularly in areas with steep slopes and intense rainfall	To develop an integrated geospatial model combining the USLE, RUSLE equations with GIS.	How can the USLE and RUSLE equations be effectively integrated with GIS to develop a geospatial soil erosion prediction model?
2	Predicting soil erosion rates and identifying erosion "hotspots" is a critical challenge in environmental management. While various models exist, they often lack the accuracy and spatial resolution needed to pinpoint specific areas of high risk and assess the stability of sediment sources.	To predict the soil erosion rate and develop erosion hotspot susceptibility map and validate the result with sediment yield and field data.	What is the spatial distribution of soil erosion risk in the Miklajung Siwalik zone?
3	Identifying the main environmental and anthropogenic factors that strongly influence soil erosion is crucial for developing effective prevention and mitigation strategies. While it's widely accepted that a combination of natural and human-driven elements contributes to soil loss, the specific dominant factors	To identify the main environmental and anthropogenic factors that influence soil erosion most strongly in the Miklajung Siwalik zone.	What are the main environmental and anthropogenic factors that influence soil erosion most strongly in the

	can vary significantly by location and time.		Miklajung Siwalik zone?

1.4 Scope and Significance of Present Study

Scope

The study was conducted in the eastern region Siwalik hill located in the Morang district Miklajung Gaupalika. This study will focus on soil erosion in the mountainous regions of central Nepal. The study was conducted with duration of 6 months ranging from April 2025 to September 2025, which involves Planning and Preparation, Data Collection and Analysis, Model Development and Report Preparation and Submission. The data used in the research span from 2000 to 2024 provided by the department of Hydrometeorology Dharan regional office. This research will impact the people living in the foothills of the Himalayan range specially in the Siwalik range of Nepal. The study uses quantitative analysis of satellite imagery and GIS data along with the field sampling and testing of the sample in Laboratory

Significance

The study has analyzed the impact of rainfall intensity and land-use changes on soil erosion but will not include the effects of wind erosion. This study is driven by the need to develop a parsimonious, accurate, and scalable erosion prediction model suitable for data-limited and topographically complex regions. By integrating the well-established USLE and RUSLE models with GIS, the project seeks to develop robust soil loss susceptibility maps of the Miklajung Siwalik zone. The erosion susceptibility maps generated through this research will serve as practical tools for local government agencies, development planners, and natural resource managers to prioritize soil conservation efforts, mitigate disaster risks, and promote sustainable land management in the region. Furthermore, the study contributes to the broader scientific understanding of soil erosion processes in the Himalayan foothills under the impacts of climate change, land use transitions, and anthropogenic pressures. The research could also be used in further study of the Siwalik range

1.5 Project Organizations

This academic project seeks to predict the soil erosion rate and develop erosion hotspot susceptibility maps and validate the result with sediment yield and field data.

The approach involves detailed analysis of the site using tools like ArcGIS, field visit for the sample collection combined with the lab testing of the sample testing. The project follows a manuscript format with six chapters. Here's a brief overview of the content structure for each chapter.

- **Chapter 1** introduces the general background, problem statement, aims & objectives, and scope of the research. It also presents the organization of the project.

- **Chapter 2** provides a detailed literature review of state-of-the-art research in Soil Erosion.
- **Chapter 3** includes the detailed explanation about the study area and all required data collection and acquisition.

- **Chapter 4** includes the detailed explanation about overall methodological framework and procedures for project. discusses the major achievements and results of project & comparison of results and necessary interpretations and general discussion of the findings.

- **Chapter 5** discusses the major achievements and results of project & comparison of results and necessary interpretations and general discussion of the findings.

- **Chapter 6** presents conclusions and Recommendations including limitations & applicability.

- **Appendices:** Appendix A shows the Sieve Analysis and Hydrometer Test result, Appendix B shows the Field Visit Photographs, Appendix C shows the Sample Collection Photographs, Appendix D shows the Coordinates of Sampling Hotspots, Appendix E shows the Laboratory Testing Photographs, and Appendix F shows the Properties soil samples.

Chapter 2: Literature Review

2.1 Introduction to Soil Erosion and Theoretical Aspects

Soil erosion is considered one of the most significant global environmental and agricultural problems, leading to land degradation, declining agricultural productivity, and disruption of ecosystem services(Webster, 2005). This erosion, driven by natural and anthropogenic forces, threatens ecosystems and agricultural sustainability globally. Empirical models like RUSLE, USLE, and process-based tools (WEPP, EUROSEM) dominate erosion prediction, yet face limitations in cross-scale adaptability, high-resolution parameterization, and validation (Borrelli et al., 2021; Epple et al., 2022). RUSLE remains widely applied (17.1% of studies), leveraging factors such as rainfall erosivity (R), soil erodibility (K), slope (LS), cover (C), and conservation practices (P) (Fernández et al., 2023). However, global syntheses reveal critical gaps: underrepresentation of wind/tillage erosion, regional disparities (e.g., Central Asia, Africa), and inconsistent validation (Borrelli et al., 2021). Also, the Global Applications of Soil Erosion Modelling Tracker (GASEMT) found only 58% of studies doing any validation, with most not being calibrated to data of the region studied, limiting their practical usefulness. Emerging technologies (LiDAR, Sentinel-2A) now enable finer-resolution inputs (10 m DEMs, NDVI) to enhance model accuracy (Fernández et al., 2023).

Nepal occupies a large part of central Himalayas, and more than 80% of the land area is mountainous and still tectonically active (Bastola et al., 2019). (Koirala et al., 2019; Raya, 2023; Siwakoti, 2000) reports Nepal's severe soil erosion, averaging 25 tons/ha/year, totaling 369 metric tons annually with the middle mountains experience the highest erosion (38.4 tons/ha/year), driven by heavy rainfall, runoff, land degradation, and poor conservation practices. The erosion rates of Siwalik Zone far exceed global averages (10-15 Mg/ha/yr), driven by monsoons, weak sedimentary geology, and unsustainable land use (Dahal, 2020; Ghimire et al., 2013b). RUSLE applications in Nepal highlight anthropogenic impacts irrigated croplands lose soil 2–3 times faster than forests (Joshi et al., 2023) but suffer from coarse resolutions and limited calibration (Aryal et al., 2023). Recent advances in geospatial data (Sentinel-2A, DEM) and machine learning (ML) offer pathways to refine RUSLE's predictive capacity by integrating high-resolution inputs (10 m bands, NDVI) and addressing class imbalances (Fernández et al., 2023).

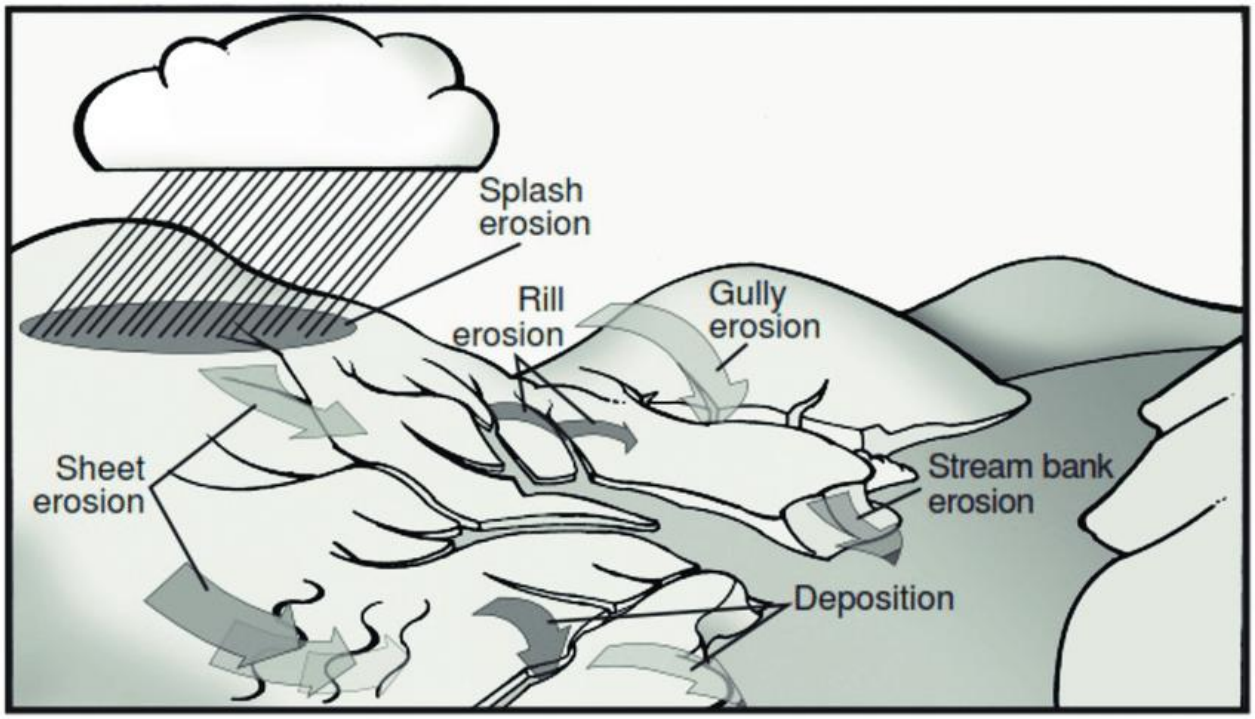

Figure 2.1: A Schematic Representation of Erosion, Displaying Commonly Used Terminology for Identifying the Elements of Soil Erosion (Firoozi & Firoozi, 2024).

2.1.1 Erosion Causes, Effects and Mitigation

Erosion causes and causative factors

Erosion can also be caused due to the movement of the water which sweep away the soil material and can also be caused due to the wind effect. Erosion may be caused by Landslides which may happen when the shear stress on a slope surpasses the shear strength of the materials comprising them. Cracks such as faults, cleavages, and similar features can reduce the strength of the slope materials, impacting the overall stability of the slope. Some of the materials that form slopes are already weak due to presence of organic stuff and clays. Even hard materials like rocks can get weak due to processes like weathering and hydrology. When minerals in clays get wet, they can lose their cohesion. Rocks can also break into pieces because of freezing and thawing or temperature changes and these factors play important role in erosion.

Erosion is complex phenomena influenced by various factors. The rainfall and wind are primary triggers responsible for erosion throughout the world. Among the various causes geological, morphological, physical and human causes are four primary causes of landslides globally (Highland & Bobrowsky, 2008). Geological formations characterized by shared,

jointed, or fissured materials are also predisposed to landslides, as these fractures create pathways for the redistribution of stress. Moreover, the orientation of geological discontinuities, such as bedding planes, schistosity, faults, unconformities, and contacts, can significantly influence landslide occurrence. Another contributing factor is the contrast in permeability and stiffness among different geological materials. Tectonic and volcanic activities, glacial rebound, erosion from intense rainfall and runoff, subterranean processes like soil saturation and piping, vegetation loss, and weathering patterns all contribute to the initiation and progression of landslides. The impact of temperature fluctuations on slope stability is significant. Thawing and freezing triggered by varying temperatures can lead to inducing volume changes in materials and weathering. Further, human activities like road construction and deforestation have a profound and intricate role in the occurrence of landslides. Moreover, mining activities can induce ground subsidence and alter the distribution of subsurface stresses, directly influencing the integrity of slopes. Artificial vibrations resulting from construction or industrial operations have the capacity to propagate through the ground, accelerating processes of slope destabilization. Following is the list of landslide causative factors considered by various researchers (Acharya, 2018).

- Geomorphological factors: elevation/altitude, relative relief, slope, aspect, general curvature (plan, profile), tangential curvature, longitudinal curvature, cross-section curvature, roughness index, topographic wetness index, stream power index, stream transportation index, slope length, diagonal length.
- Geological factors: lithology (texture, weathering), fault density, distance from faults / lineaments.
- Soil factors: soil factors include depth, drainage and hydraulic conductivity, permeability, porosity, inner texture, surface texture, slope, stoniness, effective thickness etc.
- Land use/cover factors: land cover, normalized difference vegetation index, forest (type, age, diameter, and density of timber), road density, distance from road.
- Climatic factors: annual total rainfall, annual maximum rainfall, average annual rainfall.
- Hydrological factors: river density, distance from river.

Effects of Erosion

Erosion can have a range of significant effects, impacting both the natural environment and human communities. Followings are some of the notable effects of erosion.

- **Loss of agricultural land:**

  Erosion can pose an indirect threat to human life, causing decrease in agricultural output, especially in densely Siwalik areas.

- **Property Damage:**

  Erosion can damage or destroy hydropower dams, roads, bridges, and other infrastructure, leading to economic losses and displacement of communities.

- **Environmental Changes:**

  The movement of large volumes of soil and rock can alter the landscape, reshape river channels, and impact ecosystems. This can result in changes to natural habitats and watercourses.

- **Displacement of Soil and Debris:**

  Erosion can transport soil, rocks, and debris downslope, potentially burying areas below. This displacement can lead to long-term changes in the affected terrain.

- **Disruption of Transportation:**

  Roads and transportation networks can be disrupted or blocked by landslides, causing difficulties in mobility and transportation of goods.

- **Impact on Water Bodies:**

  Erosion can lead to change in the composition of the downward moving water and can affect the downstream infrastructure, especially in water resource infrastructure.

- **Economic Consequences:**

  The damage to agricultural output, loss of property, and disruption to economic activities can have long-lasting economic consequences for affected regions.

- **Social and Psychological Impact:**

  Communities affected by erosion may experience social and psychological challenges, including loss of livelihoods, and the need for relocation.

- **Environmental Degradation:**

  soil erosion and degradation, affecting the quality of soil and water resources in the affected areas.

Mitigation Strategies for Minimizing Landslide Impacts

To mitigate the impact of landslides, several strategies can be employed. The Vulnerability to landslide hazards depends on factors like location, human activities, land usage, and the occurrence frequency of landslides. To lessen the effects of landslides on both people and structures, one approach is to completely avoid areas prone to landslide hazards. Alternatively, measures such as restricting, prohibiting, or imposing specific conditions on activities in hazard-prone zones can also be effective. Local governments play a pivotal role in minimizing landslide consequences by enforcing laws and rules on land usage. Individuals can proactively reduce their vulnerability by becoming informed about the historical hazard record of a particular site and seeking information from local planning and engineering departments. Consulting professionals such as engineering geologists, geotechnical engineers, or civil engineers is another crucial step, as they can accurately assess the hazard potential of both developed and undeveloped sites. Avoiding building on steep slopes and in locations where landslides have already occurred, as well as improving slope stability, can further reduce the likelihood of landslides. Techniques like preventing groundwater from accumulating within the landslide mass and Safe Catching through strategies such as (1) landslide cover with an impervious membrane, (2) draining surface and groundwater from the landslide, (3) catch ditches, and (4) reduce use of surface irrigation, can effectively boost stability etc. (Highland & Bobrowsky, 2008).

Additional methods such as employ biotechnical slope protection techniques involving vegetated composite soil-structure structures, utilizing materials like soil nails and nets, along with grass seeding can be adopted. Construction on steep slopes and existing erosion prone area must be avoided and employ landslide maps and area definitions to minimize hazard impact. Through these measures, the effects of erosion can be significantly mitigated, safeguarding both people and infrastructure. To effectively minimize the risk due to erosion, commonly employed approaches include limiting development in erosion-prone areas, enforcing and adhering to construction codes, and safeguarding existing developments.

2.1.2 Soil Erosion Mechanism & Types

Typically, soil erosion is differentiated in water erosion, wind erosion, tillage erosion and soil loss due to crop harvesting (“harvest erosion”). As the names indicate, the different erosion

types are differentiated by the main driver. For water erosion the main driver is water (e.g. precipitation, snow melt) and its erosion forms are further separated into sheet erosion, rill erosion, gully erosion. Wind as the main driver for wind erosion causes different kinds of soil transport such as creeping, saltation and suspension, depending on particle size. Tillage erosion depends on the implements used during soil tillage (e.g. moldboard plough, chisel plough) which leads to a translocation of the soil during the tillage activity. Soil loss due to crop harvesting occurs during the harvest of crops when the harvested product is in direct contact with the soil (e.g. sugar beet, potatoes; Understanding the physical processes involved in water erosion is crucial for comprehending how water interacts with the soil, leading to various forms of erosion. These mechanisms include splash erosion, surface runoff, and subsurface flow, each contributing uniquely to the degradation of soil and alteration of landscapes.

Soil Erosion Mechanisms

A. Splash erosion: dynamics and initial consequences

Splash erosion marks the initial interaction between rainfall and the soil surface, setting the stage for subsequent erosion processes It involves the impact of falling raindrops creating small craters in the soil surface, which can eject soil particles up to 60 cm away from the point of impact (Eekhout & de Vente, 2022). To contextualize these dynamics, consider the Loess Plateau, where studies have documented splash erosion rates contributing significantly to the annual soil loss, emphasizing the severity of this process in arid to semi-arid environments (Li et al., 2022).

- **Fundamental dynamics:**

Splash erosion represents the initial interaction between raindrops and the soil surface, a critical first step in the broader process of water erosion. When raindrops hit the soil, they do so with a force that is capable of dislodging soil particles, an effect amplified by the kinetic energy contained within each raindrop. This kinetic energy is primarily a function of the raindrop's size and velocity; larger and faster-moving droplets exert more force, causing greater disturbance to the soil surface. As raindrops impact the soil, they break apart the aggregates that make up the soil structure, effectively loosening particles and reducing the overall cohesion of the soil layer(Wu et al., 2019)

The energy released upon impact causes soil particles to be ejected from the soil surface, which can be spread over a small area depending on the intensity of the rain. This dispersion is critical as it marks the beginning of further soil erosion processes, setting a foundational stage that can exacerbate more severe erosion types like sheet and rill erosion. The mechanics of splash erosion are thus not only about the movement of soil but also about the alteration of the soil's physical structure, which affects its susceptibility to subsequent erosive forces(Dunkerley, 2021).

Fig.2.2 illustrates the dynamics of splash erosion under two scenarios: (a) Undisturbed State, where soil particles are dislodged by rain impacts on a soil surface protected by an organic litter layer, facilitating water infiltration and reducing surface runoff; (b) After Litter Clearance, showing increased erosion and overland water flow due to the absence of protective litter, which leads to enhanced soil water runoff and reduced infiltration, exacerbating splash erosion by 2–12 times. This comparative visualization underscores the importance of maintaining natural litter layers to mitigate splash erosion effects (Luo et al., 2021)(Alavinia et al., 2019; Balabathina et al., 2020).

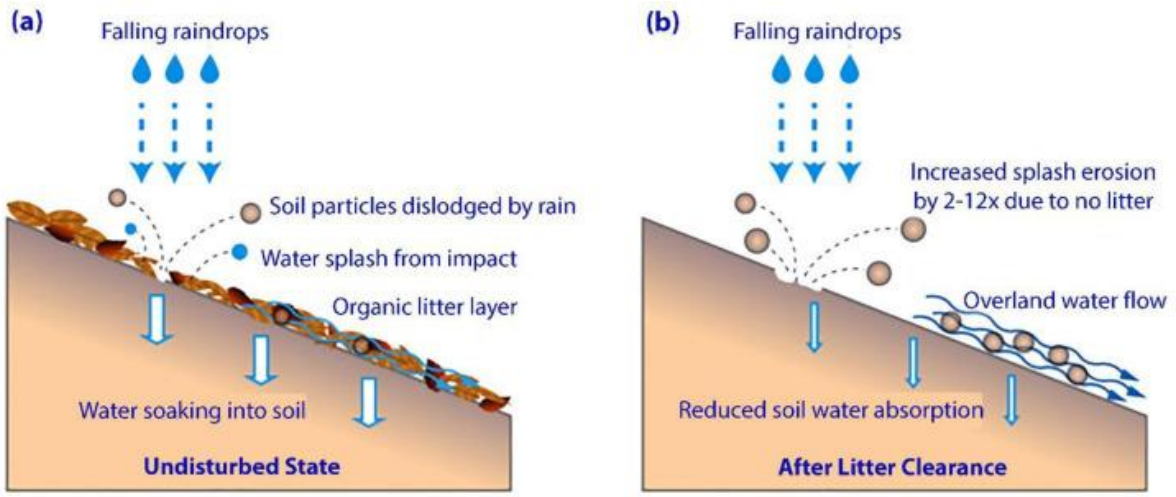

(a) Raindrop impact on bare soil (b) Soil particle displacement resulting from the impact

Figure 2.2: Dynamics of Splash Erosion Under Different Environmental Conditions (Firoozi & Firoozi, 2024).

Considering these dynamics and consequences, understanding and mitigating splash erosion is essential for effective soil conservation strategies. Techniques such as maintaining vegetation covers to intercept raindrops and employing mulching to protect the soil surface can significantly reduce the impact of splash erosion, thereby preserve soil integrity and prevent more severe erosion downstream (Aregai & Biedemariam, 2019; Prancevic & Kirchner, 2019).

B. Surface runoff: dynamics and erosion progression

Surface runoff can rapidly gather speed and energy, especially on sloped surfaces, dramatically increasing its potential for soil erosion (Owens, 2020) . As water accumulates more volume from rainfall, it gains enough force to detach and transport soil particles, leading to significant erosional impacts (Spiekermann et al., 2022) . Empirical data from the Ethiopian Highlands indicate that surface runoff on steep agricultural lands can result in erosion rates exceeding 200 tons per hectare annually, underscoring the critical need for effective soil conservation measures in such regions (Smith et al., 2020) .

In addition, a pertinent example is observed in the Mississippi River Basin, where research has quantified splash erosion rates, noting that it can displace soil particles up to 60 cm from the impact site, contributing significantly to the overall erosion dynamics in this region (Wilkes et al., 2019) . This exemplifies how splash erosion serves as a precursor to more severe erosion forms, reinforcing the need for early soil conservation interventions.

- **Flow dynamics:**

Surface runoff is a critical process in the hydrological cycle, especially concerning soil erosion. It occurs when the volume of water on the ground surpasses the soil's ability to absorb and infiltrate it. Several factors contribute to this phenomenon, including soil saturation, soil type, and the intensity of precipitation. Once the infiltration capacity of the soil is exceeded, excess water begins to flow over the land surface. This runoff can rapidly gather speed and energy, especially on sloped surfaces, dramatically increasing its potential for soil erosion (Bhat et al., 2019) .

As surface runs off travels over the soil, it exerts shear stress on the soil surface, detaching and carrying away soil particles. The erosive power of runoff is significantly amplified as it accumulates more soil particles. This not only increases the volume of sediment being

transported but also the abrasive force of the runoff, enabling it to erode the soil more efficiently. The dynamics of surface runoff are thus not static; they evolve as the water moves across the landscape, gaining momentum and erosive capability, which can lead to more severe erosional forms if not properly managed (Onet et al., 2019; Wang et al., 2024) .

Table-2.1 illustrates various environmental and anthropogenic factors that influence runoff, detailing their specific effects on water erosion processes. This table aids in understanding how different factors contribute to the intensity and volume of runoff, ultimately impacting erosion rates.

Table 2.1: Factors Affecting Runoff and Their Impact on Erosion.

Factor	**Description**	**Impact on Runoff and Erosion**
Soil Type	Different soils have varying infiltration rates and moisture retention capacities.	Soils with high clay content tend to have lower infiltration rates, leading to higher runoff and increased erosion.
Land Slope	The gradient of the land effects water flow velocity.	Steeper slopes lead to faster runoff, increasing erosion potential.
Vegetation Cover	Plants and their root systems help stabilize soil and absorb water.	Dense vegetation reduces runoff by increasing water infiltration and stabilizing the soil, thus decreasing erosion.
Land Use Practices	Human activities that alter the landscape, such as agriculture and urban development.	Poor land management practices like deforestation and uncontrolled urban expansion increase runoff and erosion rates.
Rainfall Intensity	The amount and rate of rainfall impact how much water the soil can absorb.	Heavy, intense rains overwhelm the soil's ability to absorb water, significantly increasing runoff and erosion.

- **Erosion progression:**

The progression of erosion from surface runoff is a dynamic process that often leads to the formation of rills and gullies, each representing an escalation in the severity of erosion. Rills are narrow channels that form as runoff concentrates in specific pathways, eroding the soil and deepening the channel. These rills can eventually evolve into gullies, which are much larger and deeper channels that can be several meters in depth and width. Gully erosion represents a significant geomorphological change to the landscape, leading to substantial losses of soil and changes in the land's usability (van Leeuwen et al., 2019; Yuan et al., 2022) .

Gullies not only transport large amounts of sediment downstream but also disrupt agricultural activities and can lead to further degradation of the landscape, such as increased runoff and reduced water infiltration across the broader area. This form of erosion is particularly destructive as it creates feedback mechanisms that exacerbate the erosive processes, leading to rapid and extensive landscape changes. The management of surface runoff is therefore crucial in preventing the initial formation of rills and the subsequent development of gullies (Bollati et al., 2019) .

- **Management implications:**

Understanding the flow dynamics and erosion progression associated with surface runoff is essential for developing effective soil and water conservation strategies. Measures such as contour plowing, the construction of check dams, and the implementation of riparian buffers can significantly reduce the velocity of surface runoff and its capacity to transport soil. Additionally, maintaining vegetation cover can dramatically decrease the impact of runoff by increasing soil roughness and promoting water infiltration, which diminishes the volume of water contributing to surface runoff (Haruna et al., 2020; Pulley & Collins, 2024) .

The effective management of surface runoff not only helps in controlling soil erosion but also enhances water quality and preserves the integrity of aquatic ecosystem by reducing sedimentation and nutrient loading in water bodies (Du et al., 2022).

C. Subsurface flow: underground movement and impact on soil stability

Subsurface flow, though less visible, significantly influences soil stability and erosion beneath the surface. This type of water movement involves the infiltration of water into deeper soil layers and its flow through the soil matrix. The impacts of subsurface flow are critical, as they can lead to the weakening of soil structure and increase susceptibility to various forms of erosion. This section discusses the underground movement of water and its implications for soil stability, highlighting the importance of managing subsurface flow to maintain landscape integrity.

- **Underground movement:**

Subsurface flow, the movement of water through the soil profile beneath the surface, plays a significant yet often understated role in the process of erosion. Unlike surface runoff, subsurface flow involves water that infiltrates the soil and moves through the soil layers, following paths of least resistance such as soil pores and cracks. This movement is critical for recharging groundwater but also has implications for soil stability and structure (Negese, 2021; Urbina et al., 2019) .

As water permeates and moves through the soil, it can lead to the leaching of essential nutrients, which are washed away from the root zones of plants, decreasing soil fertility and agricultural productivity. Moreover, the continuous movement of water through these subsurface pathways can gradually weaken the structural integrity of the soil (Medina et al., 2021).. Over time, this weakening can lead to more severe structural failures, such as collapses or slumps, particularly in soils that are susceptible to subsidence or those with high silt or sand content, where cohesion is less robust (Ávila et al., 2021; Giupponi et al., 2019) .

- **Impact on soil stability:**

The implications of subsurface flow for soil stability are particularly pronounced in areas characterized by high rainfall or rapid snowmelt. In such environments, the volume of water moving through the soil can dramatically increase, exacerbating the processes of leaching and structural weakening. Permeable soils, such as sandy or loamy soils, are especially vulnerable as their large pore allows for more rapid water movement (Guzzetti et al., 2022; Zhu & Zhang, 2019).

This increased movement not only destabilizes the soil from within but also makes the surface layer more susceptible to other forms of erosion. For example, when the subsurface layers are weakened, the overlying soil can become more prone to sliding, especially on slopes during heavy rain events. Furthermore, the alteration of subsurface water dynamics can affect the surface runoff patterns, often leading to increased erosion elsewhere as water exits the soil system more quickly, carrying soil particles with it (Fan et al., 2019; Sene, 2024) .

- **Managing subsurface flow for soil stability:**

Managing the effects of subsurface flow is crucial for maintaining soil stability and preventing erosion. Techniques such as the installation of drainage systems can help control the direction and speed of subsurface water movement, reducing the risk of soil saturation and subsequent structural failures. Additionally, incorporating organic matter into the soil can improve its structure, increase its water-holding capacity, and reduce the speed of water movement through the soil, thereby mitigating the risk of nutrient leaching and structural weakening (Raimondi et al., 2023; Stephens et al., 2021) .

In agricultural settings, practices such as crop rotation and the use of deep-rooted plants can help maintain soil structure and reduce the vulnerability of the soil to subsurface flow-induced erosion. These plants can help bind the soil more effectively and absorb excess water, reducing the potential for subsurface flow to destabilize the soil (Greco et al., 2023) .

In conclusion, understanding the dynamics of subsurface flow and its impacts on soil stability is essential for comprehensive erosion management. By addressing the challenges posed by subsurface flow, land managers can enhance soil health, reduce erosion risks, and maintain the structural integrity of landscapes, particularly in environments prone to heavy rainfall and rapid hydrological changes (Fu et al., 2019) .

Soil Erosion Types

According to Origin:

a) Geological Erosion: It is a natural phenomenon and in this situation the rate of soil production is equal to the rate of soil loss. It is a slow process that is offset by the creation of soil because of natural weathering. In terms of agriculture, its consequences aren't significant. Topographical features such as valleys, channels and other features are formed by this process.

b) Accelerated Erosion: It is also known as anthropogenic erosion or erosion caused by humans. In this instance, the rate of soil production is not equal to the rate of soil loss in general. In comparison to geological erosion, this is a quick process. Soil fertility on agricultural land is depleted because of accelerated erosion. Anthropogenic factors such as deforestation, slash-and-burn agriculture, extensive ploughing, etc. lead to this sort of erosion.

According to Erosion Agents:

a) Water Erosion: It is a three-step natural occurrence that involves soil particle dissociation, transport and deposition. The first two processes influence the amount of soil eroded, whereas the third phase defines how the eroded material is distributed across the landscape. There would be no deposition if there was no erosion. Soil detachment and transport can be caused by both raindrops and water runoff. A single raindrop starts the erosion process by weakening and dislodging an aggregate, which eventually leads to large-scale soil erosion during heavy rainstorms. When the rate of precipitation exceeds the rate of water infiltration, runoff occurs. Water erosion is the most common type of erosion in humid and sub-humid locations with frequent rainstorms. Water erosion is further categorized based on the wide-ranging actions of water that cause erosion into-Gully erosion, Splash erosion, Interill erosion, Rill erosion, Tunnel erosion, Sheet erosion, Streambank erosion, Coastal erosion and Landslide erosion.

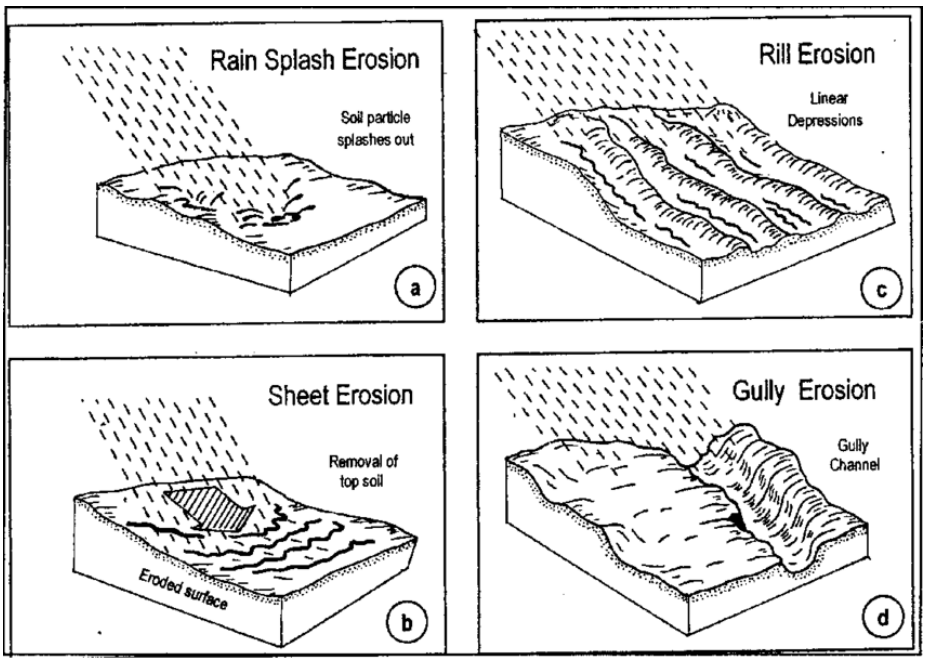

Figure 2.3: Water Erosion (Firoozi & Firoozi, 2024).

b) Wind Erosion: The removal, movement, and redeposition of soil particles by wind is known as wind erosion. It is particularly common in dry locations, where strong winds brush against various landforms, tearing them open and freeing soil particles, which are then lifted and moved in the direction of the wind. Wind erosion reduces root zone depth and water-holding capacity in shallow soils and soils with a hardpan layer. Such changes might happen slowly and go unnoticed for years, especially if the impacts are masked by tillage. Wind erosion influences not just the qualities and processes of the eroding soil, but also the nearby soils and landscapes where deposition may occur. Wind, unlike water, has the power to carry soil particles up and down slopes polluting both the air and the water. Wind erosion rates rise in the following order: arid>semiarid>dry subhumid areas>humid places. Sand dunes and mushroom rock structures which are common in deserts are the best examples of wind erosion.

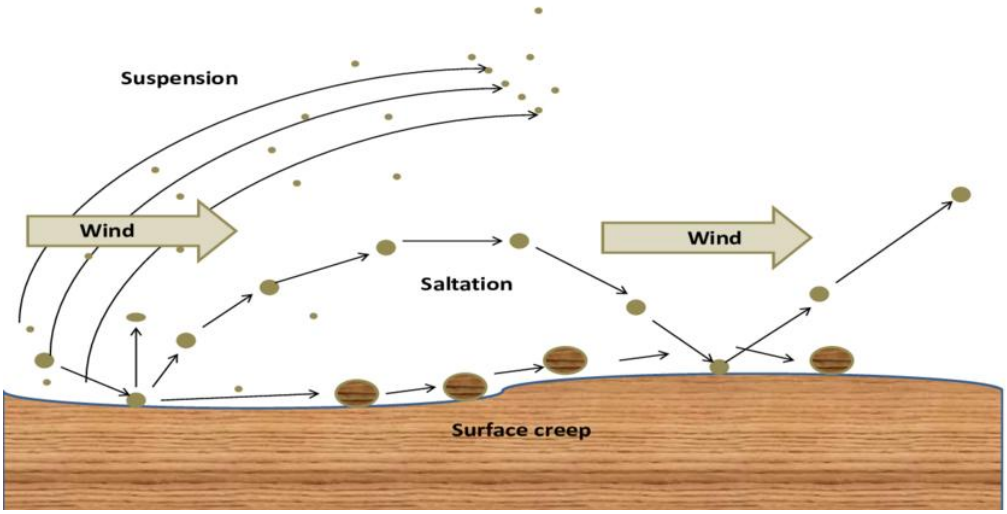

Figure 2.4: Wind Erosion (Firoozi & Firoozi, 2024).

c) Glacial Erosion: Glacial erosion, also known as glacier erosion, is widespread in cold, high-altitude environments. Soil adheres to the glacier's base when it encounters huge moving glaciers. This is eventually moved with the glaciers and as they begin to melt it is deposited in the flowing ice pieces.

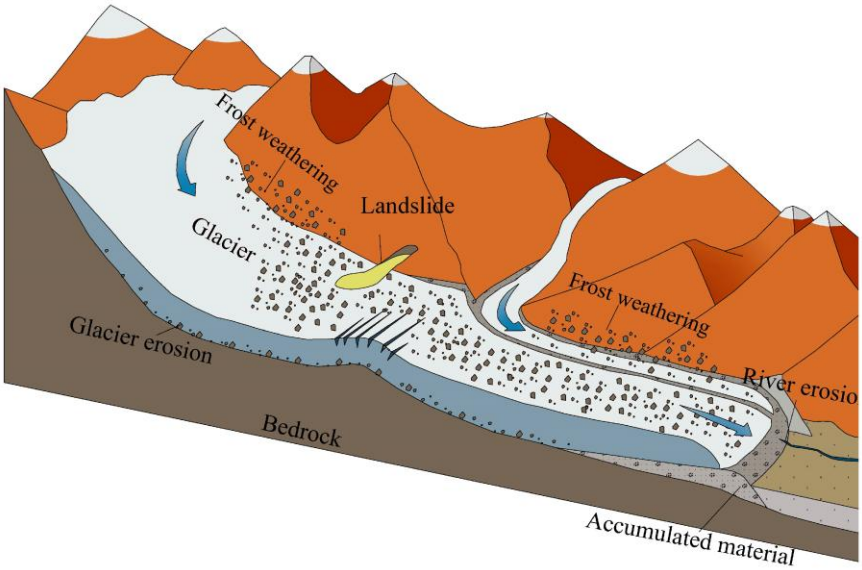

Figure 2.5: Glacial Erosion (Firoozi & Firoozi, 2024).

d) Gravitational Erosion: Even though gravity erosion is not as widespread as water erosion it can inflict significant damage to both natural and man-made buildings. It is the mass movement of soil because of gravitational force. Landslides and slumps are the best illustrations of this. While landslides and slumps happen in a matter of seconds, phenomena like soil creeps take longer to manifest.

Figure 2.6: Gravitational Erosion.

2.2 Soil Erosion Predictors

The study will follow four main predictor variables. These predictors were categorized into topographic, hydrologic, soil-related, climatic, geological, and anthropogenic factors:

1. Climatic predictor: (R-factor)

Rainfall Erosivity factor (R) can be defined as the measure of the potential ability of rainfall to cause soil erosion. It quantifies the intensity and kinetic energy of rainfall to determine the potential to detach and transport soil particles. Greater intensity and duration of rainfall result in higher potential for soil erosion. R varies with geographical location, high R-factor values are generally associated with regions experiencing frequent, intense, or prolonged rainfall, leading to greater susceptibility of soils to detachment and transport. Since rainfall patterns vary across climatic zones, the R-factor exhibits significant spatial and temporal variability, and its accurate estimation requires long-term data or the use of empirical models and erosivity maps. In soil erosion studies, the R-factor plays a crucial role in quantifying erosion risk, designing conservation practices, and informing sustainable land management strategies.

2. Soil and Lithological Predictors: Soil Erodibility (K-factor)

The K factor is the rate of soil loss per rainfall erosivity index for a specific soil, as measured in unit-plot conditions by keeping the LS, C and P factors constant at 1.0. It is a measure of the soil's capability to resist erosion, with higher values indicating higher erosion susceptibility and vice versa(282, n.d.). Thus, the K factor is in effect a lumped parameter that captures the integrated effect of the soil properties (especially physical properties like texture, structure, porosity) that influence its erosional response. These are in effect, the soil hydraulic conductivity, permeability and total water capacity, as well as any other attributes that might influence soil particle detachment and transportation due to rainfall and the ensuing runoff (282, n.d.).

3. Topographic Predictors: (LS-factor)

The dimensionless topographic factor LS comprises of the slope length (L) and slope steepness (S) factors. Wischmeier and Smith (1978) defined L as "the distance from the

point of origin of overland flow to the point where either the slope gradient (S) decreases enough that deposition begins, or the runoff water enters a well-defined channel that may be part of a drainage network or a constructed channel". Longer slopes allow greater runoff accumulation, while steeper slopes increase the shear stress of flowing water, both of which intensify soil detachment and transport.

4. Anthropogenic Predictor: (C & P-factor)

The cover and management factor (C-factor) is defined as the ratio of soil loss from a field with specific cover and management to that of a field under 'clean-tilled continuous fallow(282, n.d.). Being a ratio, it normally varies between 0 and 1.0, unless an area is more erosion-prone than the unit-plot. Lower C-factor values indicate greater protection, as dense vegetation intercepts raindrops, reduces runoff velocity, and enhances infiltration, while higher values are associated with bare or poorly managed lands. The C-factor is highly dynamic, varying seasonally with changes in crop growth stages, residue cover, and tillage practices.

The support practice (P-factor) is "the ratio of soil loss with a specific support practice to the corresponding loss with up-and-down-slope culture"(282, n.d.). It is representative of the efficacy of erosion control measures, with values close to zero suggestive of the success of a particular erosion control practice. Contouring, contour strip-cropping, terracing and stabilized waterways are some of the conservation practices recommended to reduce the P factor value of a cropland (282, n.d.). The values of P-factors range from 0 to 1. Lower values indicate greater effectiveness of conservation measures such as contour farming, strip cropping, terracing, or the use of bunds and check dams, which reduce slope length, slow runoff, and promote water infiltration. The P-factor is highly site-specific, depending on slope gradient, type of practice, and implementation efficiency.

2.3 Soil Erosion Assessment Principle and Approaches

The principles of soil erosion assessment are grounded in understanding the dynamic interaction between erosive forces, soil properties, topography, land cover, and conservation practices. At its core, erosion assessment seeks to quantify the rate at which soil is detached, transported, and deposited, primarily by rainfall and surface runoff. Frameworks such as the Universal Soil Loss Equation (USLE) and its revised forms (RUSLE) operationalize this

principle by integrating key factors: rainfall erosivity (R), soil erodibility (K), slope length and steepness (LS), land cover and management (C), and support practices (P). These models assume that erosion risk is proportional to the intensity of erosive forces and inversely related to protective measures such as vegetation cover and soil conservation practices. Modern soil erosion assessment emphasizes not only empirical and experimental approaches but also the use of geospatial technologies, hydrological models, and remote sensing to capture spatial variability and predict long-term trends. Overall, the principle highlights that accurate soil erosion assessment is essential for identifying vulnerable areas, designing effective soil and water conservation strategies, and ensuring sustainable land resource management.

Research Approaches:

1) Empirical Approaches

Empirical approaches to soil erosion assessment are based on statistical relationships between observed soil loss and environmental variables such as rainfall, soil properties, slope, land cover, and conservation practices. Unlike process-based models, which attempt to simulate the physical mechanisms of detachment, transport, and deposition, empirical models depend on experimental data and regression analysis to predict soil erosion under specific conditions. The Universal Soil Loss Equation (USLE) and its revised versions (RUSLE) are the most widely used empirical models, developed through long-term plot experiments across diverse agroecological zones. These approaches are valued for their simplicity, ease of application, and minimal data requirements, making them particularly useful for large-scale erosion risk mapping and conservation planning. However, their reliance on site-specific calibration and inability to fully capture complex hydrological and geomorphological processes limit their accuracy in heterogeneous landscapes. Despite these limitations, empirical approaches remain a cornerstone of soil erosion assessment, especially when integrated with modern GIS and remote sensing techniques for spatial analysis.

a) USLE Approach

The origin of USLE-type models was in the US to provide a management decision support tool and was based upon thousands of controlled studies on field plots and small watersheds since 1930 (Alewell et al., 2019). As with all empirical methods the model concept is not based on

process description and simulation but rather on understanding a process, capturing the confounding measurable parameters and delineating a mathematical algorithm out of the relationship between these parameters and the measured output (in this case measured eroded sediments). As such, the average annual soil loss (A) (ton/hectare/year) at any location can be estimated using USLE **(Eq. 1).**

$$A = R \times K \times L \times S \times C \times P \quad \text{…… (1)}$$

where: A (Mg ha^{-1} yr^{-1}) is the annual average soil erosion, R (MJ mm h^{-1} yr^{-1}) is the rainfall-runoff erosivity factor, K (Mg h MJ^{-1} mm^{-1}) is the soil erodibility factor, L (dimensionless) is the slope length factor, S (dimensionless) is the slope steepness factor, C (dimensionless) is the land cover and management factor, P (dimensionless) is the soil conservation or prevention practices factor. The impact of the factors R capturing the energy and amount of precipitation, K accounting for the soil parameters determining erosion potential, C describing the vegetation cover and management as well as P delineating human management intervention is directly related to our process understanding of soil erosion.

i. RUSLE Approach

The Revised Universal Soil Loss Equation (RUSLE) models erosion influenced by soil, climate, topography, and land use. Inter-rill erosion results from raindrop impact and surface runoff (Renard *'a & Freimund, 1994).The model integrates five raster-mapped factors: slope length-gradient (LS), rainfall erosivity (R), soil erodibility (K), cover-management (C), and support practices (P). These spatially and temporally variable parameters depend on external drivers. The average annual soil loss (A) (ton/hectare/year) at any location can be estimated using RUSLE **(Eq. 2),**(Avand et al., 2023):

$$A = R \times K \times LS \times C \times P \quad \text{…… (2)}$$

where R is rainfall erosivity (MJ/hectare/mm); K is the soil erodibility (ton/hectare/year); LS is the slope length and slope gradient; C is the cover management practice; and P is the conservation support or erosion control practices.

ii. MUSLE Approach

The Modified Universal Soil Loss Equation (MUSLE), developed by Williams (1975), is an extension of the USLE designed to estimate sediment yield from individual storm events rather

than long-term average annual soil loss. Unlike USLE and RUSLE, which use rainfall erosivity (R) as the driving factor, MUSLE replaces it with a runoff factor that incorporates storm runoff volume and peak discharge. The sediment yield can be estimated using MUSLE **(Eq.3)** (Zhang et al., 2009)**.**

$$Y=11.8(Q\cdot q_p)^{0.56}\cdot K\cdot C\cdot P\cdot LS \quad \text{(3)}$$

where Y is sediment yield (tons), Q is runoff volume, q_p is peak discharge, A is drainage area, and K, C, P, LS retain their definitions from USLE.

2) Machine Learning Approach

Machine learning (ML) approaches have recently emerged as powerful tools for soil erosion assessment, offering data-driven alternatives to traditional empirical models like USLE, RUSLE, and MUSLE. Unlike these equation-based models, ML techniques such as decision trees, random forests, support vector machines, artificial neural networks, and ensemble learning can capture complex nonlinear relationships between soil erosion and its controlling factors, including rainfall, soil properties, topography, land cover, and conservation practices. By applying large datasets from field measurements, remote sensing, and GIS, ML models can improve predictive accuracy and provide spatially explicit erosion risk maps. A major advantage of machine learning is its ability to adapt to diverse landscapes without requiring explicit assumptions about underlying physical processes. However, challenges include the need for high-quality training data, the potential for overfitting, and limited interpretability compared to process-based models. Despite these limitations, machine learning approaches are increasingly being integrated with geospatial technologies and hydrological models, making them valuable for large-scale erosion monitoring, conservation planning, and sustainable land management.

Chapter 3: Study Area and Data

3.1 Study Area Description

Nepal is a mountainous country located between India and China, positioned along the boundary of the Indian and Eurasian tectonic plates. The Subduction of the Indian Plate beneath the Eurasian Plate makes Nepal highly susceptible to earthquakes and the related hazard like landslides and slope failures leading to major soil loss and erosion (Okamura et al., 2015). The general topography of country characterized by high relief, complex geological structures, and extreme variation of elevation from south to North. 83% of the total area lies in hilly and high mountainous region (Acharya, 2018). This makes Nepal highly vulnerable to soil erosion and slope failure related hazards especially along the mid hill region. The Siwalik Hill is geologically fragile, steep, and prone to cascading hazards like landslide, slope instability and soil erosions. The region marked by elevation gradients approximately 144 to 2,400 Meters Above Sea Level (MASL) and underlaid by weak sedimentary rock structures like sandstone, shale and conglomerates, which are vulnerable to accelerated weathering and mass wasting processes (S. K. Ghimire et al., 2013b; Siwakoti, 2000). Fig(3.1) shows the seismo-tectonics of Nepal Himalaya, major fault systems.

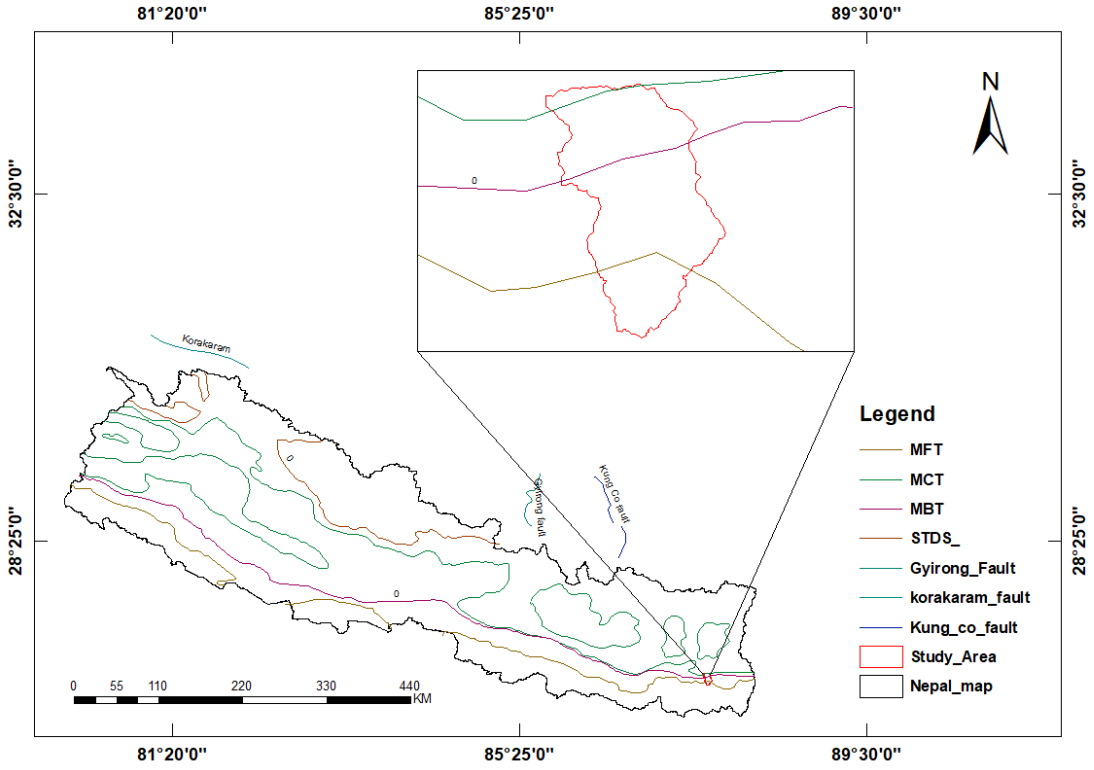

Figure 3.1: Map Showing Seismo-Tectonics of Nepal Himalaya, Major Fault Systems of Nepal and Study Area.

3.1.1 Site Location

The Bakraha watershed is selected as the study area for this work. It lies between 26° 43′ 48″ N latitude and 87° 37′ 48″ E longitude in the Morang district of Nepal. The watershed is drained by the Bakraha River, which is a monsoon-dominated perennial river originating from southern slopes of the Mahabharata Range, which is part of the sub-Himalayan hills(M. Ghimire, 2020). The Bakraha watershed lies in the Siwalik zone, underlaid by weak sedimentary rock, sand stones, and conglomerates(S. K. Ghimire et al., 2013a). The river flows southwards, crossing the Chure hills and eventually entering the Terai region before crossing the border into India(M. Ghimire, 2020). Bakraha watershed includes soil types dominated by calcaric phaeozems, eutric sambisols, eutric fulvisols, dystric regosols, (Dijkshoorn & Huting, 2009). Bakraha watershed is dominated by forest in hilly region and agricultural land in terai region. The region has very steep variation in elevation in small areas, as the elevation ranges from 144m to 2400m above sea level within 104.66 Km^2. The significant elevation difference has resulted in diverse climatic conditions ranging from subtropical warm to humid conditions. Climactically, the region's shaped by strong monsoonal rains, with an average annual precipitation of about 2,061 mm. most of which fall during June-September.

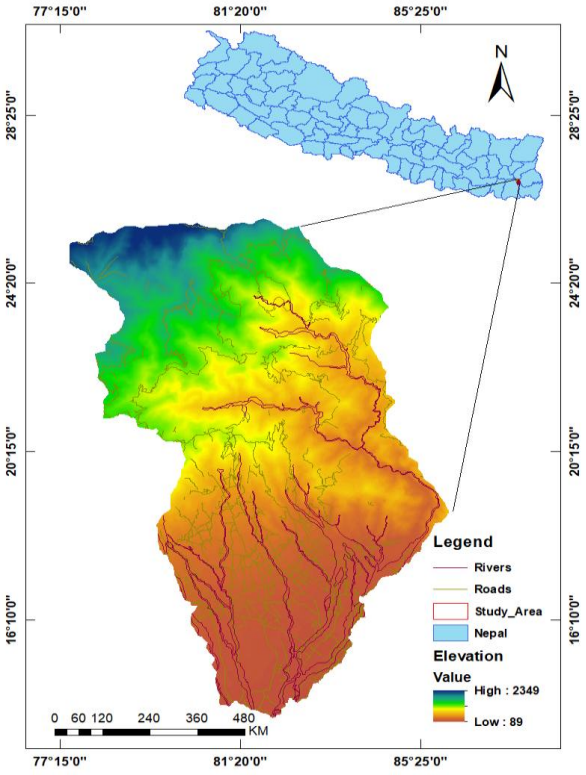

Figure 3.2: Map Showing the Study Area with Major Rivers, Roads, and Elevation.

3.1.2 Topographical and Geological setting

The overall terrain of Morang is made up of Terai plain, Siwalik Range, Mid-Hill range with an elevation difference of 2256 m (lowest: 144m and highest: 2400 m). The Siwalik Hills are geologically fragile, steep, and prone to cascading hazards like landslides, slope instability and soil erosion. The region marked by weak sedimentary rock structures like sandstone, shale and conglomerates, which are vulnerable to accelerated weathering and mass wasting processes (S. K. Ghimire et al., 2013b; Siwakoti, 2000). Bakraha watershed includes soil types dominated by calcaric phaeozems, eutric sambisols, eutric fulvisols, dystric regosols,(Dijkshoorn & Huting, 2009). Unsustainable agriculture practices create severe soil erosion and sediment shifts throughout the landscape. Moreover, regional infrastructure (such as roads and settlements) is increasingly threatened by slope failure from erosion. Fig (3.3) shows the geological description of study area including dominant soils.

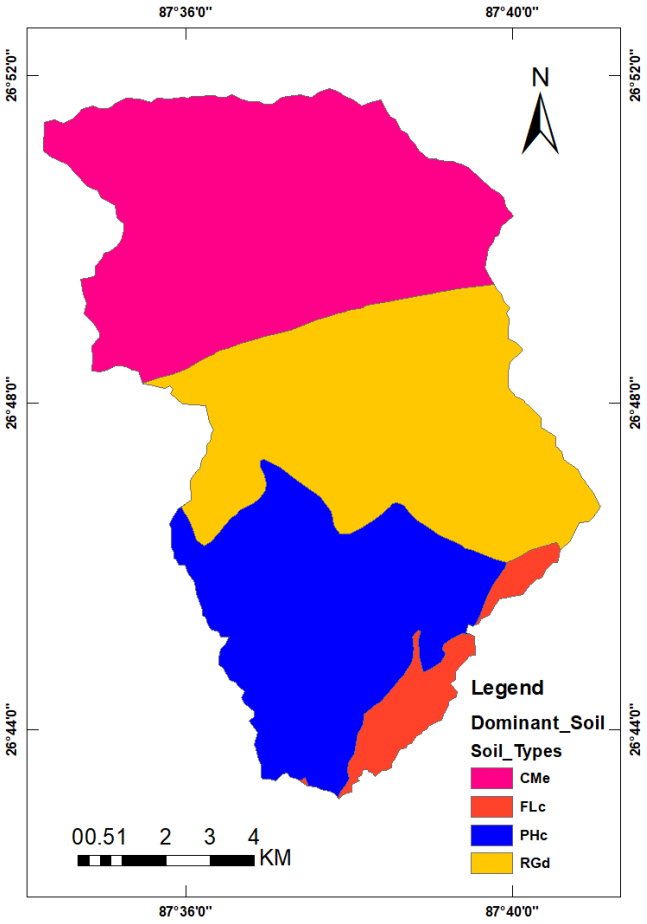

Figure 3.3: Dominant Soil Types.

3.2 Data Acquisition

Erosion is complex process. The reliability of erosion susceptibility assessment depends on sound inventory data and causative factors. Understanding the erosion causative factors and making inventory mapping are crucial steps for assessment of soil erosion. The accuracy of erosion susceptibility maps depends on reliable inventory and causal factors.

3.2.1 Erosion Hotspots & Inventories

The erosion inventory map was created using Geographical Information System (GIS) and using google earth. Fifty erosion hotspots were delineated in google earth using polygon and the kml file was imported into the GIS environment using kml to layer function.

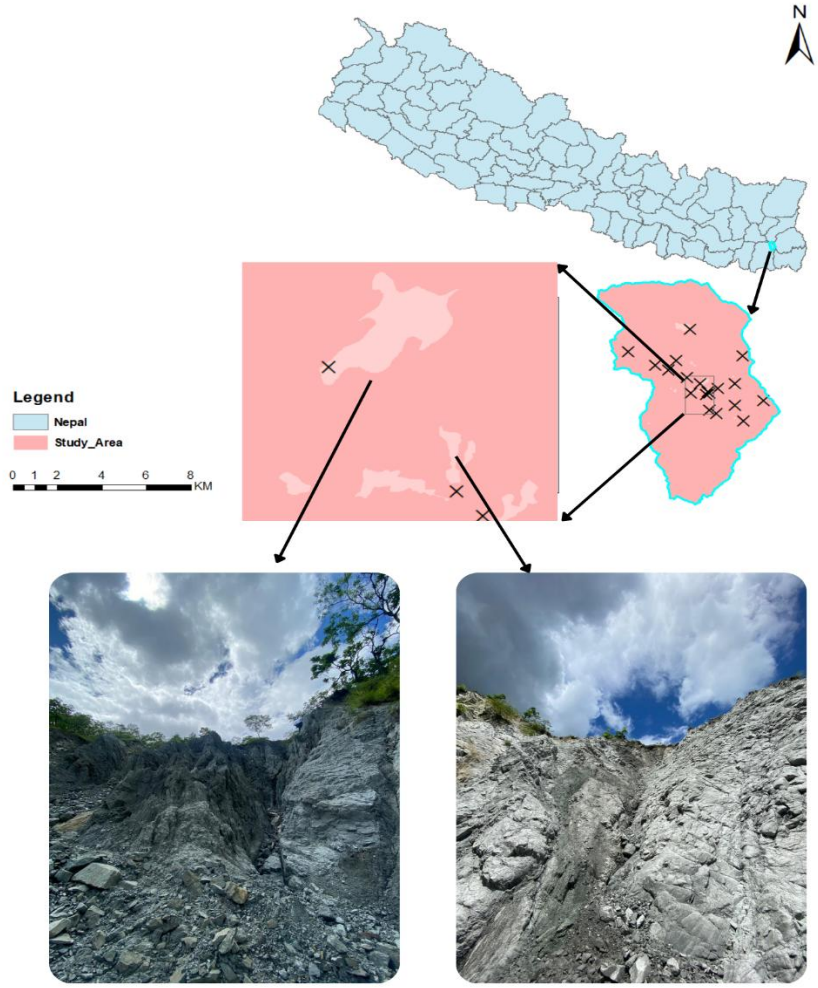

Figure 3.4: Soil Erosion Hotspots and Inventory Map.

3.2.2 Digital Elevation Model & its Derivatives

A Digital Elevation Model (DEM) is a digital representation of the Earth's surface that serves as a critical input in hydrological and soil erosion studies. DEMs not only provide elevation data but also allow the derivation of several secondary topographic attributes, commonly referred to as DEM derivatives. ASTER DEM of 12.5m resolution was used to derive its derivatives such as elevation, slope in degree, flow accumulation, fill in ARCGIS environment. Fig(3.5) shows the DEM & its derivatives of the study area.

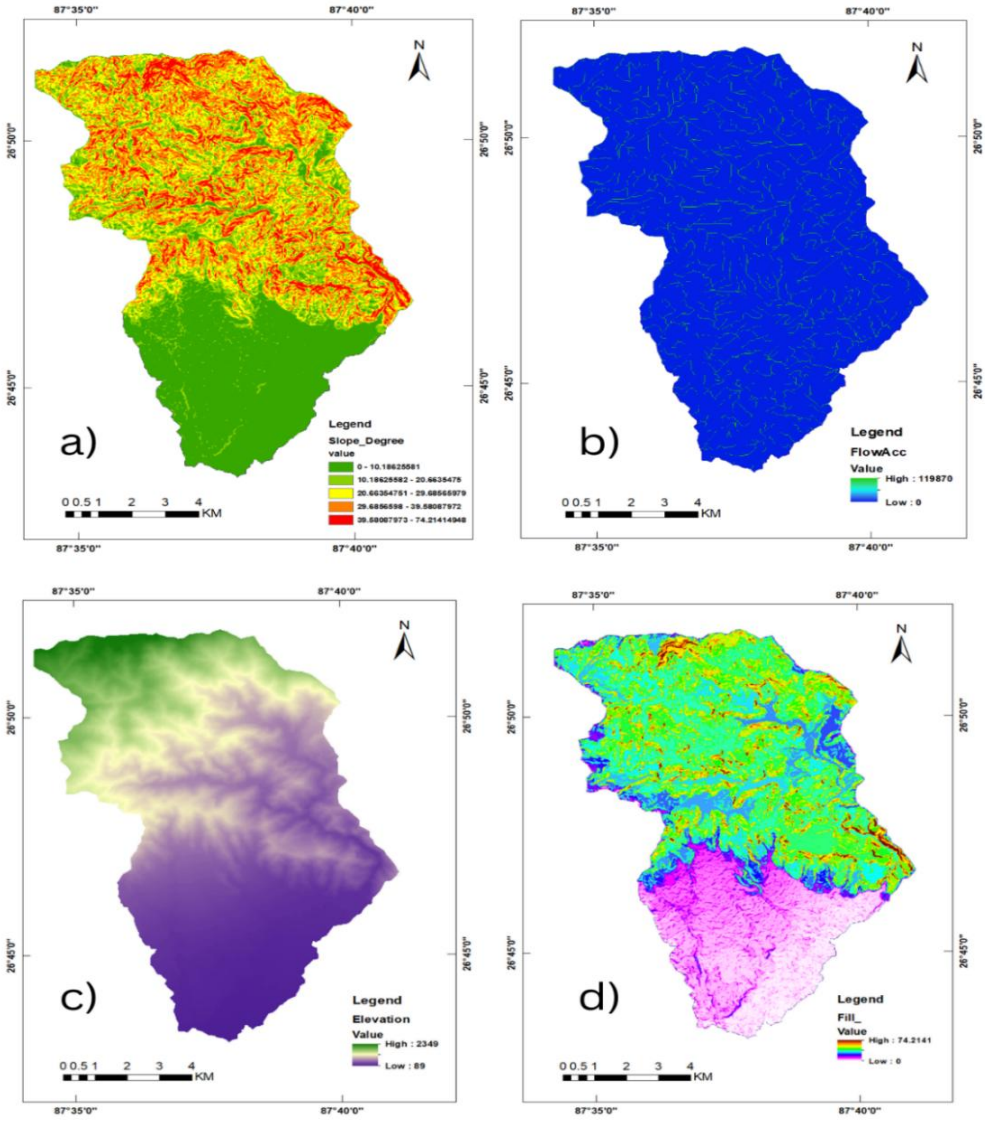

Figure 3.5: Thematic Mapping of DEM Its Derivatives (a) Slope Degree, (b) Flow Accumulation, (c) Elevation, (d) Fill

3.2.3 Normalized Difference Vegetation Index

The Normalized Difference Vegetation Index (NDVI) is one of the most widely used remote sensing indices for assessing vegetation cover, health, and dynamics, and it plays a crucial role in soil erosion studies. NDVI values range between –1 and +1, where higher values indicate dense and healthy vegetation, while lower or negative values correspond to barren surfaces, water bodies, or degraded land. NDVI map was generated in google earth engine using Landsat 8 satellite imagery. The value ranges from 0.067 to 0.089, the low value indicates that southern part of Bakraha watershed is barren surfaces, water bodies, or degraded land and the higher value indicates that northern part of watershed is dense and healthy vegetation. Fig (3.6) shows the NDVI map of Bakraha watershed.

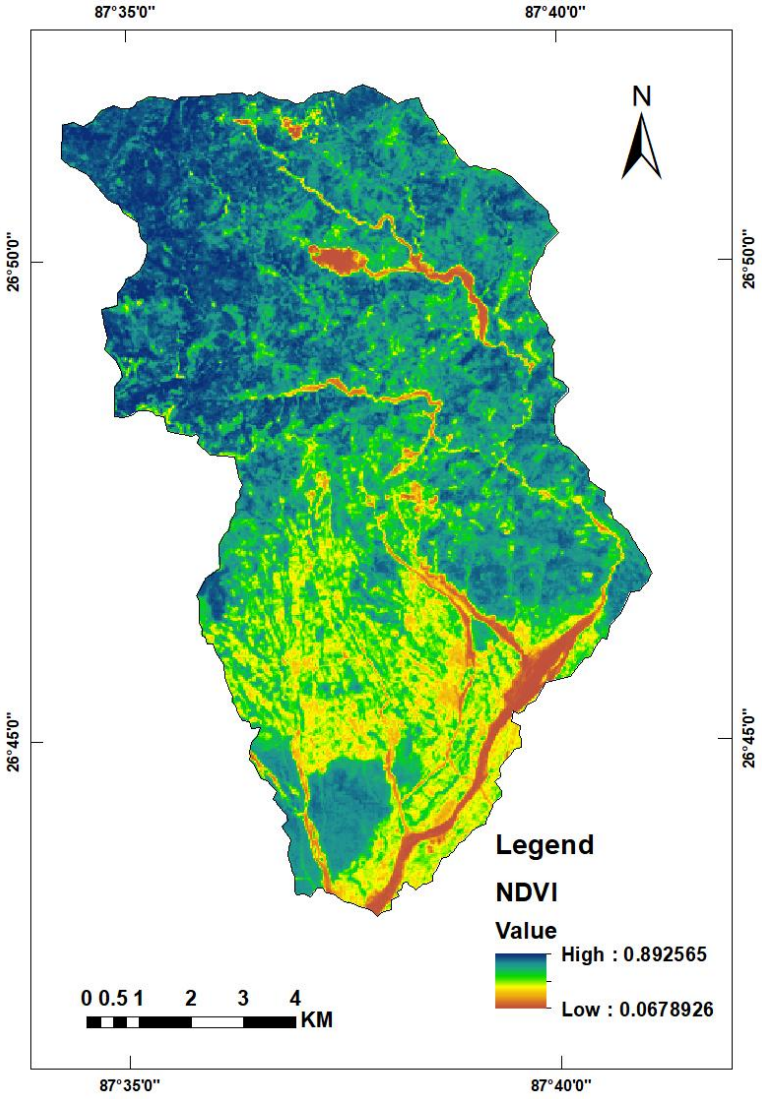

Figure 3.6: NDVI Map of Bakraha Watershed

3.2.4 Land Use & Land Cover

Land use and land cover (LULC) are fundamental concepts in environmental studies, natural resource management, and soil erosion assessment. Land cover refers to the physical characteristics of the Earth's surface, such as vegetation, water bodies, bare soil, or built-up areas, while land use describes how humans utilize this land, including agriculture, forestry, urban development, or conservation practices. A buffered Bakraha watershed was used in Google earth engine environment, and the features such as water bodies, agricultural land, forest, riverbed, grass land, bare land, and built-up areas are selected and classified with classes as 0, 1, 2, 3, 4, 5, 6 respectively. Fig (3.7) shows the LULC map of Bakraha watershed.

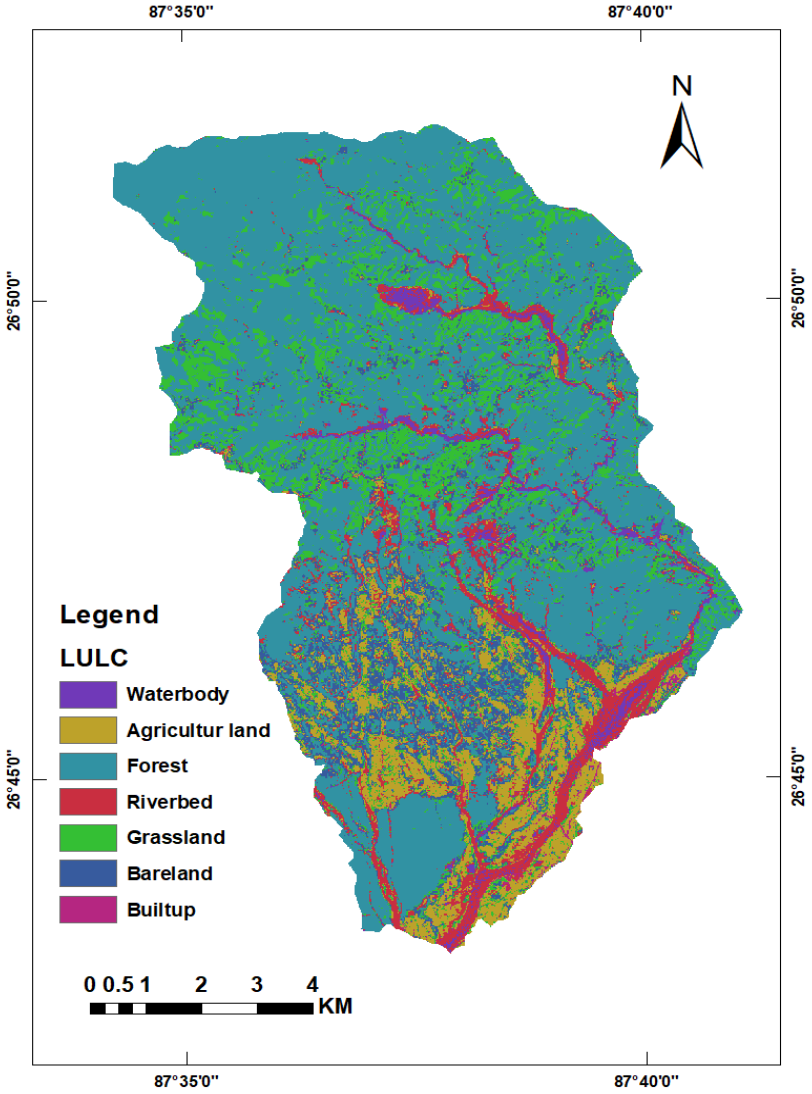

Figure 3.7: LULC Map of Bakraha Watershed.

3.2.5 Precipitation and Hydrological Data

Precipitation is the process by which water in the atmosphere condenses and falls to the Earth's surface in various forms such as rain, snow, sleet, hail, or drizzle. Precipitation data was collected as one of the key input parameters for the study, since rainfall plays a crucial role in influencing surface runoff, soil erosion, and sediment transport processes. The data was obtained from Department of Hydrology and Meteorology (DHM) Dharan, Nepal in the form of daily/monthly rainfall records for the selected stations within and around the study area. Rainfall data of total twenty rainfall stations were collected. Fig (3.8) shows the precipitation and hydrological data.

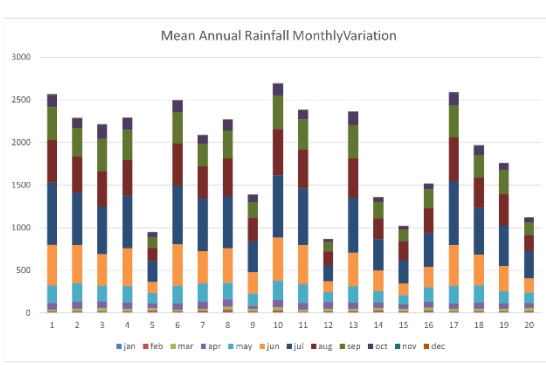

a)

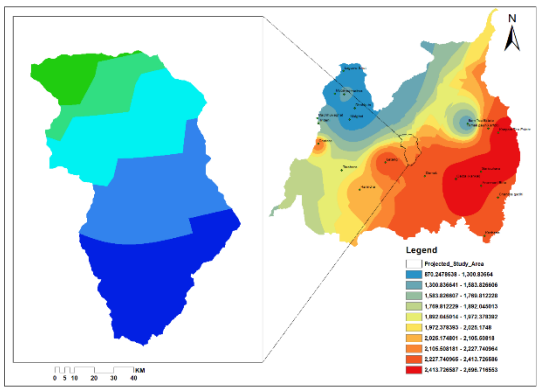

b)

S.N.	Station Name	Latitude	Longitude	Altitude (m)	AAR (mm)
1	Anarmani Birta	26.62506389	87.9885806	122	2565.801685
2	Chandra gadhi	26.570391	88.075144	95	2289.968371
3	Chatara	26.820435	87.159165	105	2217.8675
4	Damak	26.67066583	87.7031758	119	2294.096105
5	Dhankuta	26.98321944	87.3459556	1192	952.1738768
6	Gaida (kankai)	26.65688889	87.8607222	107	2497.502083
7	Harincha	26.61000889	87.3707478	93	2091.326542
8	Himali gaun(karfok)	26.88652778	88.0273889	1654	2270.610743
9	Ilam Tea Estate	26.90963889	87.9230833	1208	1395.476584
10	Kanyam Tea Estate	26.86805556	88.0783333	1570	2696.717482
11	Kechana	26.39616667	88.00375	71	2386.887337
12	Leguwa Ghat	27.15338889	87.2891944	446	870.2474012
13	Letang	26.73416667	87.5016667	256	2365.860217
14	Machhuwaghat	26.93805556	87.1547222	168	1359.789951
15	Muga	27.0500025	87.2444444	1457	1022.579286
16	pakharibas	27.04633889	87.2925	1720	1519.375
17	Sanischare	26.68972222	87.9886111	168	2589.938063
18	Tarahara	26.69881889	87.2787378	120	1970.377083
19	Tribeni	26.91424278	87.15986	146	1762.1175
20	Mulghat	26.93175	87.31969	286	1121.945641

c)

Figure 3.8: Map Showing Hydrological Data Used in This Study, (a) Histogram of Mean Annual Rainfall (b) Rainfall Intensity in Study Area, (c) Coordinates of Stations.

3.2.6 Soil Type and Properties

Soil type and properties were considered as essential datasets for the study, as they directly influence infiltration, permeability, and erodibility. The soil samples were collected from different points of study areas where erosion took place. sieve analysis and hydrometer analysis were conducted in laboratory to determine the soil textural classes and included parameters such as soil texture (proportion of sand, silt, and clay), organic matter content, and permeability. These properties were used to classify soil into different hydrological groups and to determine the soil erodibility factor (K) in erosion modeling. Understanding soil type and its physical and chemical characteristics is crucial for assessing its response to rainfall, runoff, and land use practices.

Table 3.1: Geology of Study Area and Soil Types.

Soil type		
Dominant_S	**Landform**	**Geology**
Eutic Cambisols	TM	Recent
Dystric Regosols	TH	Lower Siwalik
Calcaric Fluvisols	LV	Seti Formation
Calcaric Phaezems	LF	Shiprin Khola Formation
		Sarung Khola Formation
		Takure Formation
		Middle Siwalik

Chapter 4: Methodology

The research was conducted at Madan Bhandari College of Engineering Laboratory and Library. The data were collected from various sources. The rainfall data was collected from the Department of Hydrology and Meteorology Dharan which provided us with the rainfall data of past 20 years furthermore the DEM data was collected from ASTER, and these data were used in the GIS Software for Model development on soil erosion. The data used in the analysis are given in fig (4.1). The soil sample were collected through the field visit and were tested in the laboratory of Madan Bhandari College of Engineering, which is equipped with state-of-the-art facilities for geotechnical testing, enabling the determination of soil properties such as grain size distribution, specific gravity. These parameters are critical inputs for soil erosion and stability modeling. The laboratory provided a controlled environment for precise and reliable testing, essential for the accuracy of geotechnical assessments.

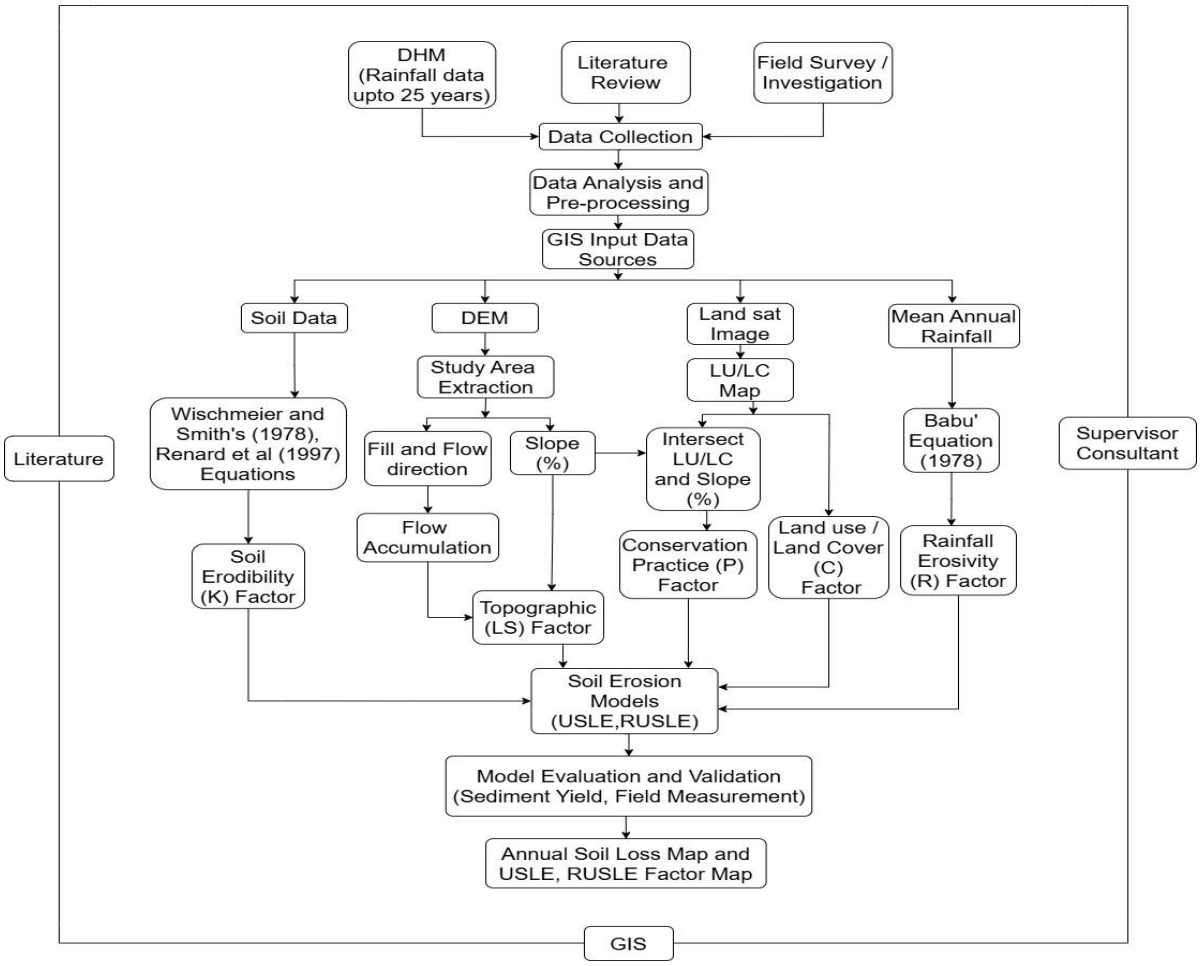

Figure 4.1: Flowchart Showing Methodological Framework of the Study.

4.1 Determination of Soil Erosion Predictors

Soil erosion predictors are the key factors and variables used to estimate the rate, severity, and risk of soil erosion in each area. They are often combined into models like the Universal Soil Loss Equation (USLE), Revised USLE (RUSLE), or more advanced simulation models.

4.1.1 R-Factor

The rainfall erosivity factor (R) describes the erosivity of rainfall at a particular location based on the rainfall amount and intensity, and kinetic energy of rainfall also reflects the effect of rainfall intensity on soil erosion. The rainfall erosivity used in the RUSLE must quantify an effect of raindrop impact and explain the amount and rate of runoff associate with rainfall and its unit is expressed in MJ mm ha^{-1} h^{-1} yr^{-1}. In this study, the rainfall map produced by data given by Department of Hydrology and Metrology was used to generate a rainfall erosivity factor. The rainfall map represents mean annual precipitation over the Study area, produced from the ground meteorological stations. The equation integrated to generate the R-factor is given by.

$$R = 38.5 + 0.35P \quad \text{..... (4)}$$

where,

R = Rainfall Erosivity Factor,

P = Mean Annual Rainfall in mm.

4.1.2 K- Factor

The soil erodibility factor (K) is a quantitative description of the inherent erodibility of a particular soil type; it is a measure of the susceptibility of soil particles to detachment and transport by rainfall and runoff. The main soil properties influencing the K factor are soil texture, organic matter, soil structure and permeability of the soil profile. For a particular soil, the soil erodibility factor is the rate of erosion per unit erosion index from a standard unit plot of 22.13 m long slope length with 9% of slope gradient. It reflects the rate of soil loss per rainfall erosivity (R) index.

In the absence of soil structure and soil permeability value, as needed in original equation, the equation provided by reference was used to estimate the soil erodibility of soil.

$$K = Fcsand * Fsi - cl * Forgc * Fhisand * 0.1317$$

where,

$$Fcsand = [0.2 + 0.3exp(-0.0256\,SAN(1 - \frac{SIL}{100}))]$$

$$Fsi - cl = \left[\frac{SIL}{CLA + SIL}\right]^{0.3}$$

$$Forgc = \left[1.0 - \frac{0.25\,C}{C + \exp(3.72 - 2.95\,C)}\right]$$

$$Fhisand = \left[1.0 - \frac{0.70\,SN1}{SN1 + exp(-5.51 + 22.9\,SN1)}\right]$$

where, SAN, SIL and CLA are % sand, silt and clay, respectively; C is the organic carbon content; and SN1 is sand content subtracted from 1 and divided by 100.

- $Fcsand$ = it gives a low soil erodibility factor for soil with coarse sand and a high value for soil with little sand content.
- Fsi-cl = it gives a low soil erodibility factor with high clay to silt ration
- Forgc = it is the factor that reduces soil erodibility for soil with high organic content.
- Fhisand= it is the factor that reduces soil erodibility for soil with extremely high sand content.

The samples were collected from different regions of the study area representing different soil types found in the region. In total, 19 samples were collected for the determination of the K factor. The sample represented the various soil types found in the region with different chemical compositions and soil structure. The collected sample were air dried for 10 days before starting the different test. the test conducted are mentioned below for the determination of the k factor.

Specific Gravity Analysis

The specific gravity was conducted using the pycnometer. Soil sample of wt. 300 gram was taken in a pan passing through 4.75mm sieve. The weight of the pycnometer was measured and then the sample was placed in the pycnometer and weight again and then the pycnometer was filled with water and then the weight was measured again. The test was performed for all 19 samples.

Where,

W1 = Weight of empty pycnometer

W2 = Weight of pycnometer + dry soil

W3 = Weight of pycnometer + soil + water

W4 = Weight of pycnometer + water

The specific gravity of soil solids (Gs)

$$Gs = \frac{(W2-W1)}{(W2-W1)-(W3-W4)} \quad \text{..... (5)}$$

Sieve Analysis

Sieve analysis is a mechanical method of determining the particle size distribution of coarse and medium-grained soils (sand and gravel, particles > 0.075 mm). It involves passing soil through a set of sieves arranged in decreasing mesh size and recording the percentage retained on each.

The sample was air-dried and then weighing and sieving were performed. The air drying was achieved by drying at room temperature for a week. The air-dried sample was weighed and sieved successively on sieves starting with the largest. sieves are clean before use. A nest of ten sieves, the lower being 75-micron and the upper approximately 4.75mm according to Specification given in IS for Test Sieves.

For the sieve analysis 1 kg of sample was taken and then the sample was shaked using shaker for 10 minutes then the sample retained at each pan was measured. The calculation table is given in Appendix A.

Hydrometer Analysis

Hydrometer analysis is a laboratory test used in soil mechanics to determine the particle size distribution of fine-grained soils (silt and clay fractions smaller than 0.075 mm or 75 microns), which cannot be analyzed accurately by sieve analysis.

For the test 40 gm of the oven dry soil sample passing through 75-micron sieve was taken after removing soluble salts and organic matter if any. It was then mixed with 4% solution of dispersing agent (sodium metaphosphate) in water to get a known amount of suspension by

volume and stirred well. The suspension was again mixed using Electric mixer with dispersing cup and Following stirring with mixer, the suspension which is made up to 1000 ml in the measuring cylinder is turned end to end for even distribution of particles before the time 'T' begins to be measured. The hydrometer readings were recorded at regular intervals as indicated in the data sheet. From the data obtained the particle size distribution curve is plotted in the semi-logarithmic graph sheet along with the dry sieve analysis results. The calculation sheet is given in Appendix A.

Corrections (Individual):

Meniscus Correction (C_m): Since the suspension was opaque, the readings will be taken at the top of the meniscus while the actual should be from the bottom of the meniscus. It is constant for a hydrometer (Always positive).

Temperature Correction (C_t): If the temperature is less than 27 ℃, the correction is negative and vice versa. Temperature should be measured from starting till end of the tests at regular intervals and are averaged. Then it is compared with the standard temperature (27 ℃). Dispersion Agent Correction (C_d): Addition of calgon always increases the specific gravity of the specimen. Hence, this correction is always negative.

4.1.3 LS -Factor

Length and steepness factors (LS) are topographic factors that describe the combined effect of slope length (flow length) and the slope gradient i.e. longer and steeper the slope, then higher the risk of erosion. The length and steepness factor (LS) in RUSLE is calculated as the product of slope length (L) and slope steepness (S), reflecting the topographic influence on erosion, with LS values indicating relative loss compared to reference condition. To depict LS factor topographic data from DEM was used to derive LS factor, and then, the DEM was used for slope analysis as well as flow accumulation in the ArcGIS platform using spatial tool along with the following equation:

$$LS = ((FlowAccumulation * CellSize)/22.13)^{0.4} * (sin((0.01745)/0.09))^{1.4}$$

The value of m varies between 0.2 to 0.5, we have adopted 0.4 in our study. Slope% is the slope in percentage

4.1.4 C- Factor

Cover Management Factor (C) is the representation of the effect of land cover (such as forest, cropland, bare soil) and management practice (tillage, mulching) on erosion rates that influence the susceptibility of soil erosion by water. The cover management factor (C factor) quantifies the effects of land use and management practices on soil erosion. It is influenced by parameters like vegetation cover, soil biomass, and rough surface complicating accurate estimation. NDVI map was generated in google earth engine using landsate-8 satellite imagery and NDVI map was generated using following equation in ArcGIS environment.

$$\text{C Factor } = 0.407 - 0.5953 \times NDVI$$

Negative value of C factor was reclassified in positive value using reclassify function in ArcGIS

4.1.5 P-Factor

The P factor represents the effect of soil conservation practices that reduce the erosive power of surface runoff. It compares soil loss with a given conservation practice to soil loss with straight up-and-down slope farming (which is taken as P = 1).

Support practice factor indicates the rate of soil loss according to the various cultivated lands. There are contours, cropping, and terrace as its methods and it is important factor that can control the erosion. The P values range from 0 to 1, where the value 0 represents a very good anthropic erosion resistance facility and the value 1 indicates a non-anthropic resistance erosion facility. The DEM was used as a spatial analysis tool to calculate the slope in percentage, and calculated slope was reclassified into five classes as shown in table below. The reclassified slope raster map was converted into polygon, then the polygon values were merged into five different classes. The P-Factor values are assigned based on the classified slope percentage and contouring as shown in table below.

Table 4.1: P Factor Values for Slope as Per Agricultural Practice

Slope (%)	Conservation Support Practices (P Factor)		
	Contouring	Strip Cropping	Terracing
0.0–7.0	0.55	0.27	0.10
7.0–11.3	0.60	0.30	0.12
11.3–17.6	0.80	0.40	0.16
17.6–26.8	0.90	0.45	0.18
>26.8	1.00	0.50	0.20

4.2 Soil Erosion Assessment Models

4.2.1 USLE

The origin of USLE-type models was in the US to provide a management decision support tool and was based upon thousands of controlled studies on field plots and small watersheds since 1930(Alewell et al., 2019). As with all empirical methods the model concept is not based on process description and simulation but rather on understanding a process, capturing the confounding measurable parameters and delineating a mathematical algorithm out of the relationship between these parameters and the measured output (in this case measured eroded sediments). As such, the average annual soil loss (A) (ton/hectare/year) at any location can be estimated using USLE as **(Eq. 6).**

$$A = R \times K \times L \times S \times C \times P \quad \text{..... (6)}$$

where: A (Mg ha^{-1} yr^{-1}) is the annual average soil erosion, R (MJ mm h^{-1} yr^{-1}) is the rainfall-runoff erosivity factor, K (Mg h MJ^{-1} mm^{-1}) is the soil erodibility factor, L (dimensionless) is the slope length factor, S (dimensionless) is the slope steepness factor, C (dimensionless) is the land cover and management factor, P (dimensionless) is the soil conservation or prevention practices factor. The impact of the factors R capturing the energy and amount of precipitation, K accounting for the soil parameters determining erosion potential, C describing the vegetation cover and management as well as P delineating human management intervention is directly related to our process understanding of soil erosion.

(Babu, 1978), The modified equation will be used to determine the Rainfall erodibility (R) factor using **(Eq. 7).**

$R = 831.626 + 3.877P$ …….……..……..……..……..…….... (7)

Where R is the MJ mm ha^{-1} h^{-1} yr^{-1} and P is the annual precipitation (mm).

The soil erodibility (k) factor will be calculated using the (WH Wischmeier & DD Smith, 1978) equation **(Eq. 8).**

$K = [2.1 \times 10^{-6} \times M^{1.14} \times (12\text{-}a) + 0.0325 \times (b\text{-}2) + 0.025 \times (c\text{-}3)]$ ….……..……... (8)

Where,

$M = (SIL + VFS) \times (100 - CLA)$ ….……..……..……..……..…… (9)

SIL + VFS: Mass fraction (%) of silt and very fine sand, i.e. particles with sizes between 2 and 100 µm. CLA: Mass fraction (%) of clay particles (< 2 µm). a: soil organic matter mass fraction (%); b: soil structure code, 1 (very fine granular), 2 (fine granular), 3 (medium or coarse granular), 4 (blocky, platy or massive); c: profile permeability class, and 1 (rapid), 2 (moderate to rapid), 3 (moderate), 4 (slow to moderate), 5 (slow), 6 (very slow) respectively,(WH Wischmeier & DD Smith, 1978).

(DK Mccool & LC Brown, 1987), Equation will be used to calculate the slope factor (L) using the **(Eq. 10).**

$L = \left(\frac{\lambda}{22 \cdot 13}\right)^{m}$ ….……..……..……..……..……..……..…… (10)

Where,

$m = \frac{\beta}{1+\beta}$ ….……..……..……..……..……..……..…….... (a)

$\beta = \frac{\left(\frac{\sin\theta}{0.0896}\right)}{3(\sin\theta)^{0.8}+0.56}$ ….……..……..……..……..……..……...……(b)

λ is the slope length (m).

(DK Mccool & LC Brown, 1987), Has also given the mathematical Equation to calculate the slope steepness factor (S) as **(Eq. 11)**

$S = 10.8 \sin\theta + 0.03$ $(For\ slopes < 9\%)$

$S = 16.8 \sin\theta - 0.5 \; (For\ slopes \geq 9\%)$ …………………………………………… (11)

$S = 3\,(sin\,\theta)\,0.8 + 0.56\;(For\ \lambda < 4.5\,m)$

Where,

θ is the slope angle.

The land use/ land cover factor (C) and conversation practice (P) will be computed from the available literature.

4.2.2 RUSLE

The Revised Universal Soil Loss Equation (RUSLE) models erosion influenced by soil, climate, topography, and land use. Inter-rill erosion results from raindrop impact and surface runoff (Renard *’a & Freimund, 1994).The model integrates five raster-mapped factors: slope length-gradient (LS), rainfall erosivity (R), soil erodibility (K), cover-management (C), and support practices (P). These spatially and temporally variable parameters depend on external drivers. The average annual soil loss (A) (ton/hectare/year) at any location can be estimated using RUSLE **(Eq. 12),** (Avand et al., 2023):

$A = R \times K \times LS \times C \times P$ …………………………………………………………….. (12)

where R is rainfall erosivity (MJ/hectare/mm); K is the soil erodibility (ton/hectare/year); LS is the slope length and slope gradient; C is the cover management practice; and P is the conservation support or erosion control practices. Wischmeier and Smith's equation can be used to calculate the soil erodibility factor **(Eq.13):**

$100K = 2.1M^{1.14} \times 10^{-4} \times (12 - \%OM) + 3.25(S-2) + 2.5(P-3)$…………….... (13)

Where, K is the soil erodibility, M is particle size (% silt + % very fine sand) (100% clay), OM is the organic matter content (%), and S and P, are the soil structure and permeability classes, respectively.

(Renard *’a & Freimund, 1994),method can be used to calculate annual rainfall erosivity from monthly and annual average of rainfall data **(Eq. 14):**

$$R = 0.7397F^{1.847}, F < 5 \text{ mm}$$
$$and\ R = 95.77 - 6.081F + 0.477F^2, F > 55 \text{ mm} \quad \text{..... (14)}$$
$$F = \sum_{i=1}^{12} P_i^2 / \bar{P}$$

Where, F is the modified index value, P_i, is average monthly precipitation (mm), P is average annual precipitation (mm), and R is rainfall erosivity (MJ/ha/mm). Some have estimated C using NDVI (Avand et al., 2023). The vegetation cover can be determined from Landsat satellite images from the USGS website (https://earthexplorer.usgs.gov/). Parameter C was obtained for each pixel with **(Eq. 15).** Further, LS can be incorporated with gradient, slope length and shape to determine sediment yield (Avand et al., 2023):

$$\text{C Factor } = 0.407 - 0.5953 \times NDVI \quad \text{.....(15)}$$

4.3 Model Evaluation & Validation

Assessing and validating the generated model is a challenging endeavor. Model evaluation examines how well a predictive model performs and the quality of its results. A common approach involves a confusion matrix, which reveals true and false counts in predictions. The model's overall performance can be assessed using the Receiver Operating Characteristic (ROC) curve, a technique applied in this study as well. It is a commonly used graphical representation that provides a clear and intuitive way to assess the accuracy of classification (Regmi et al., 2014). It shows the relationship between sensitivity (true positive) and 1-specificity (false positive), allowing easy visual evaluation. The ROC curve is determined by AUC, which measures the accuracy of training and validation sets. It ranges from 0.5 to 1, with a value greater than 0.5 indicating the model's validity and acceptability (Acharya, 2018; Chen et al., 2019). According to Amare (Amare et al., 2021), based on AUC ML- model can be categorized as Table 4.2 and The Precision, Recall, F1- score, and Accuracy of model computed as given in Table 4.3.

Figure 4.2: Illustration of Receiver-Operating Characteristic (ROC) Curve

[Source: (Acharya, 2018)]

Table 4.2: Model Classification Based on AUC (After Amare Et Al., 2021).

SN	AUC (%)	Model classification
1	AUC < 50	Very poor, unacceptable
2	50 ≤ AUC < 70	Poor, unacceptable
3	70 ≤AUC < 80	Good acceptable
4	80 ≤ AUC < 90	Very good
5	≥ 90	excellent

Table 4.3: Formula for Calculation of Model Performance.

SN	Performance matric	Formula
1	Precision	$\frac{TP}{TP + FP}$
2	Recall	$\frac{TP}{TP + FN}$
3	F1-score	$2 * \frac{Precision * Recall}{Precision + Recall}$
4	Accuracy	$\frac{TP + TN}{TP + TN + FP + FN}$

[Where, TP: True Positives, TN: True Negative, FP: False Positive, and FN: False Negative]

4.4 Tools & Software

With the rapid progress in computer science and internet technology, a plethora of tools and software has emerged to cater to diverse needs. While some are tailored for specific tasks, others offer multi functionality. In this study, we employed two distinct types of software: (1) GIS, which aided in the preparation and visualization of spatial data, (2) Google Earth Engine, which enables the creation and processing of data through a range of publicly available earth observatory software, and (3) Microsoft excel for tabular data calculation and handling.

Chapter 5: Results and Discussion

5.1 Soil Erosion Predictors

The prediction of soil erosion in this study was primarily governed by a set of key biophysical and management factors, consistent with the framework of the USLE/RUSLE model. Among these, rainfall erosivity (R) emerged as a dominant predictor, as higher rainfall intensity directly increased detachment and transport capacity of soil particles. Soil erodibility (K) was another important predictor, reflecting the role of intrinsic soil properties such as texture, organic matter, and structure in determining susceptibility to erosion. Topographic predictors derived from the DEM, particularly slope length and steepness (LS), showed a strong influence on spatial variability of erosion risk, with steeper slopes exhibiting disproportionately higher soil loss. Vegetation-related predictors, particularly NDVI and land use/land cover (LULC), effectively captured the protective role of surface cover, where dense vegetation significantly reduced predicted erosion, while agricultural and barren lands were associated with higher soil loss. The support practice factor (P) further highlighted the role of management interventions such as contouring and terracing in reducing erosion rates. Overall, the combined influence of these predictors demonstrated that soil erosion is a multifactorial process, with climate, soil properties, topography, vegetation, and management practices interacting in complex ways. The relative importance of each predictor in this study underscores the need for site-specific conservation strategies, with priority given to high-risk zones characterized by steep slopes, erodible soils, and sparse vegetation cover.

5.1.1 Erosivity Rainfall (R) Factor

value The R factor map of the Bakraha watershed is shown in Figure (5.1) was created using rainfall from different precipitation stations which depicted spatial variability in R value, in between 689.91 and 829.83 MJ/mm/ha/h/year. Lowest was observed in the Northern part of the watershed while highest was observed in the Southern part of the watershed. Lowest value indicates less intense rainfall to erode soil particles such that Northern part experiences less erosive rainfall whereas, highest value indicates Southern part of the watershed experiences the most erosive rainfall with greater risk of soil loss.

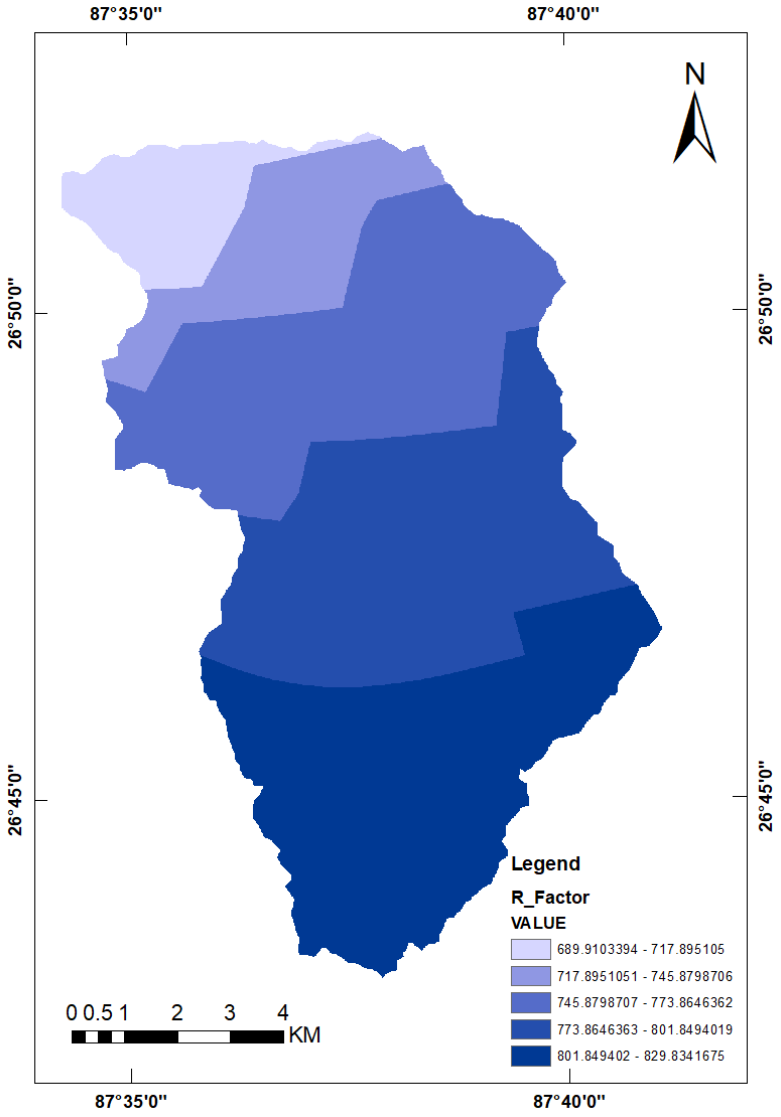

Figure 5.1: Map Showing R-Factor of Watershed.

5.2.2 Soil Erodibility (k) Factor

Soil erodibility factor map was created with the help of experimental data and soil map of the Nepal generated by NARC, Nepal. The K-value for each map unit was calculated, and it ranged from lowest 0.0138491 ton/ha/MJ/mm to highest 0.0222801 ton/ha/MJ/mm in the watershed which is shown in Figure (5.2). Erodibility factors for different soil types available within watershed are assigned and shown in table (5.1). The higher K-values indicate very fine sand, and a large amount of silt and clay which makes the soil susceptible to erosion, as it retains more water but can also easily be detached by water. Lower K-values indicate that they are

more resistant to soil erosion. The collected soil samples from watershed are characterized as Sand.

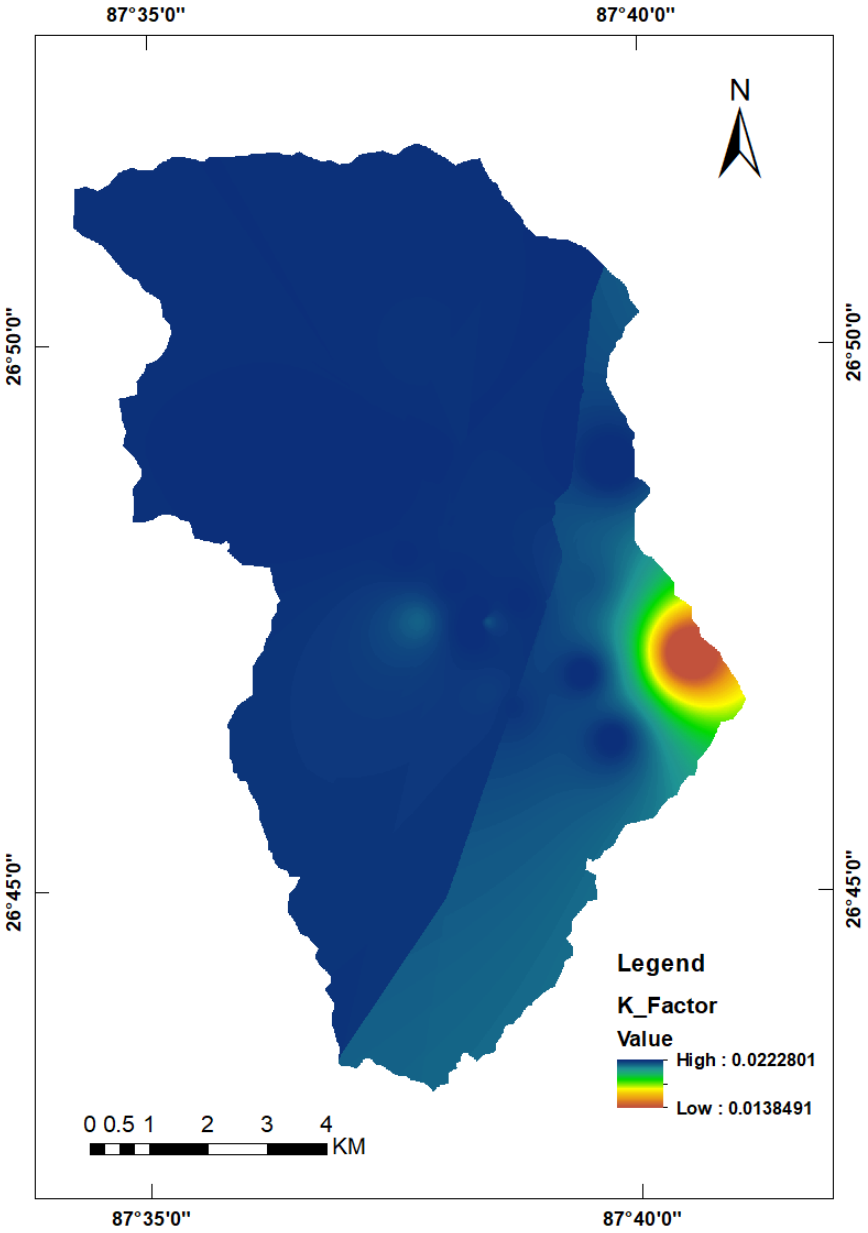

Figure 5.2: Map Showing K-Factor of Watershed.

Table 5.1: Erodibility Factors for Different Soil Types Available Within Watershed.

Name of Hotspots	Latitude	Longitude	Organic matter (%)	k-factor
A_1	26.801	87.627	3.10	0.02207842
A_2	26.797	87.635	2.85	0.022087217
A_3	26.794	87.646	2.93	0.022091808
A_4	26.791	87.629	2.71	0.02150495
B.B	26.818	87.59	3.10	0.022064557
B_1	26.79	87.639	2.70	0.022280822
B_2	26.791	87.641	2.77	0.021700136
B_3	26.792	87.64	2.76	0.022213463
B_4	26.778	87.645	2.63	0.022021779
B_5	26.78	87.641	2.54	0.02190848
K_1	26.786	87.675	3.02	0.013848704
K_2	26.797	87.657	2.98	0.021713486
K_3	26.832	87.629	3.01	0.022027379
K_4	26.815	87.662	2.79	0.02219173
K_5	26.783	87.657	2.90	0.022164599
K_6	26.773	87.662	2.56	0.022145895
S_1	26.812	87.62	2.79	0.022159111
S_2	26.809	87.607	2.94	0.022115475
S_3	26.806	87.615	3.09	0.022073331

5.2.3 LS-Factor

The LS factor is the combined result of two factors such as slope length(L) and slope steepness(S). Slope length and gradient are the important variables in soil erosion modeling, in calculating the transport capacity of surface flow. In our study, LS factor value ranged between 0-137.19 for USLE and 0-69.5774 for RUSLE, shown in Figure (5.3). The low value indicates flat or gently sloping terrain with short slope lengths. These areas are less prone to soil erosion whereas the value high indicates long slope lengths or steep slopes accumulating more energy to detach soil particles and consequently increasing erosion. Even moderate rainfall can cause significant amounts of soil loss in areas having higher LS value. These areas can be considered critical zones and should be prioritized for conservation. Soil erosion rates increase with increase in slope length and gradient values governed by the topography(282, n.d.).

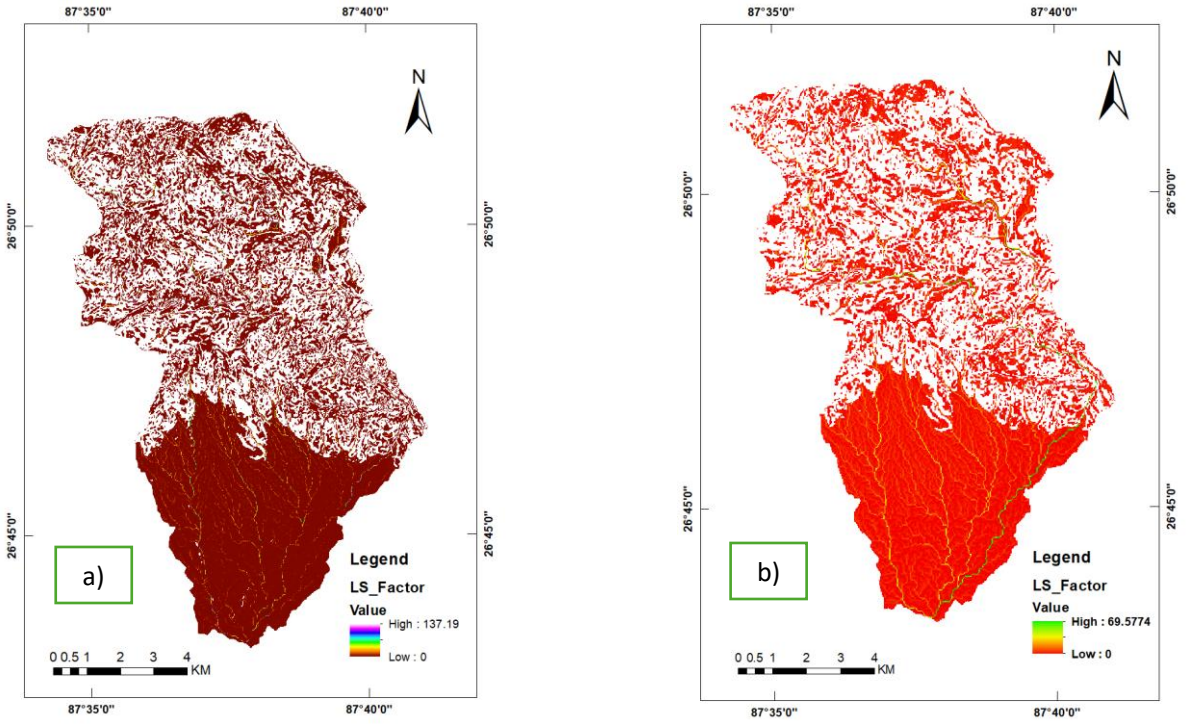

Figure 5.3: (a) LS Factor for USLE, (b) LS Factor for RUSLE.

5.2.4 Cover Management (C) Factor

The C-factor stands for the cover management factor, which shows how vegetation cover and land management techniques affect soil erosion. In other words, it describes how much erosion protection a given land cover offers in comparison to bare fallow land; a value closer to 0 denotes greater protection or they do not directly contribute to erosion, whereas a value closer to 1 denotes minimal protection (such as bare soil and bare rock) and are highly vulnerable to soil erosion. The spatial distribution of the values of crop cover factors fluctuated between 0 and 0.366584, shown in Figure (5.4). A higher value of C signifies minimal vegetation cover with high susceptibility to soil erosion, whereas a lower value indicates less susceptibility to soil erosion or no erosion.

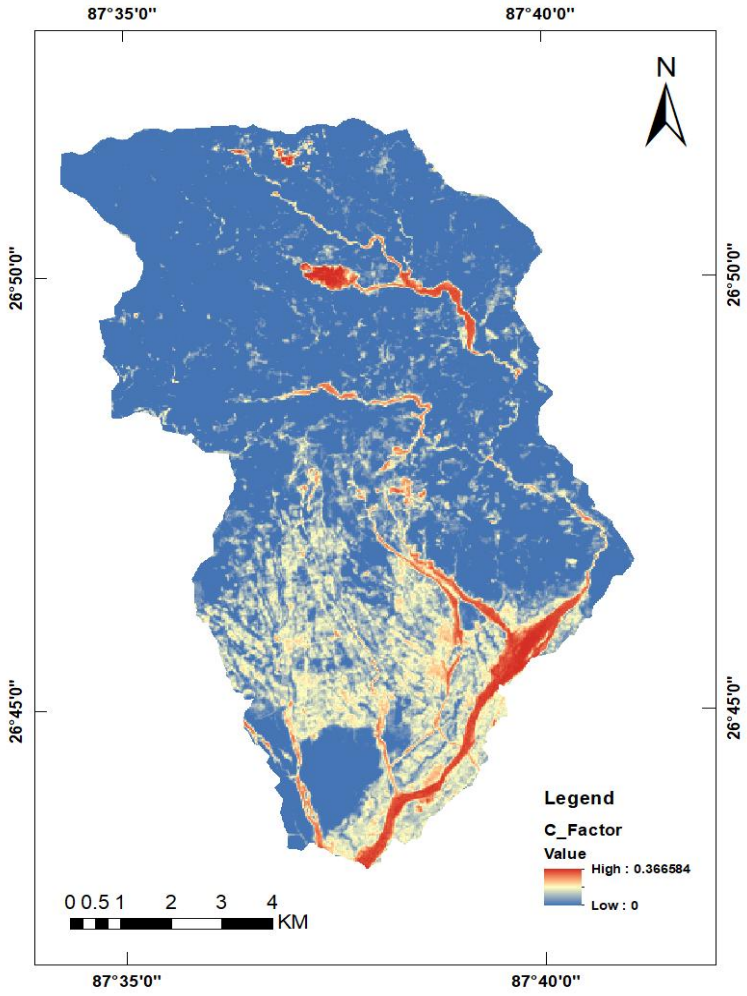

Figure 5.4: Map Showing the C-Factor of Watershed.

5.2.5 Support Practice (P) Factor

Cover Management and support practice factors are the two main key catchment specific factors to identify the rate of soil erosion, and their values vary between 0 to 1. In this study, the value of the P-factor ranged between 0.55 to 1 shown in Figure (5.5). The value 1 indicates an area with no conservation practices against soil erosion (Barren land, rock & so on) whereas the lowest value 0.55 indicates dense forest. The agricultural land with contouring, terracing, mulching, agro-forestry and so on contributes to soil erosion control measures than agricultural land with no contouring, terracing and other erosion control measures. So, P-factor is one of the most important factors that employs strategies to protect land resources.

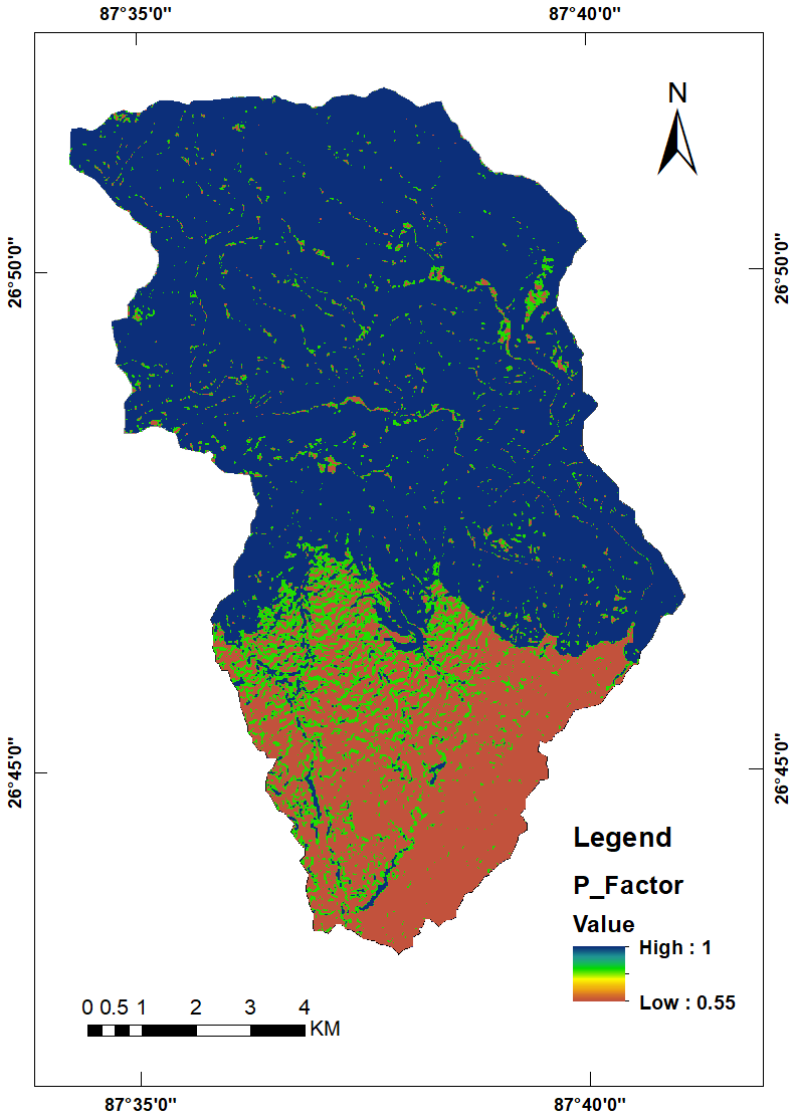

Figure 5.5: Map Showing the P-Factor of Watershed.

5.2 Soil Erosion Assessment

Soil erosion assessment is the process of quantifying the rate and extent of soil loss under varying environmental and land management conditions, with the aim of understanding its impacts and guiding conservation strategies. It is based on the principle that soil erosion is driven by the interaction of rainfall erosivity, soil erodibility, topography, land cover, and human interventions. Traditional empirical models such as the Universal Soil Loss Equation (USLE) and its revised versions (RUSLE, MUSLE) have been widely applied to estimate soil erosion, using measurable predictors to provide average annual or event-based erosion rates. In recent years, the integration of remote sensing and GIS technologies has significantly

enhanced spatial soil erosion assessment by enabling high-resolution mapping of erosion-prone areas using inputs such as DEMs, NDVI, and land use/land cover data. Moreover, emerging approaches based on machine learning and process-based models have improved prediction accuracy by capturing nonlinear relationships and physical erosion processes. Despite advances, challenges remain due to uncertainties in input data, scale dependency, and variability in local conditions. However, soil erosion assessment remains an essential tool for identifying hotspots, evaluating the effectiveness of conservation practices, and promoting sustainable land and water resource management.

The potential soil erosion map of Study Area has been produced in ArcGIS by multiplying the factor maps using USLE. It has been found that the erosion ranges from 0 to 515 t ha^{-1} yr^{-1} for the entire study area.

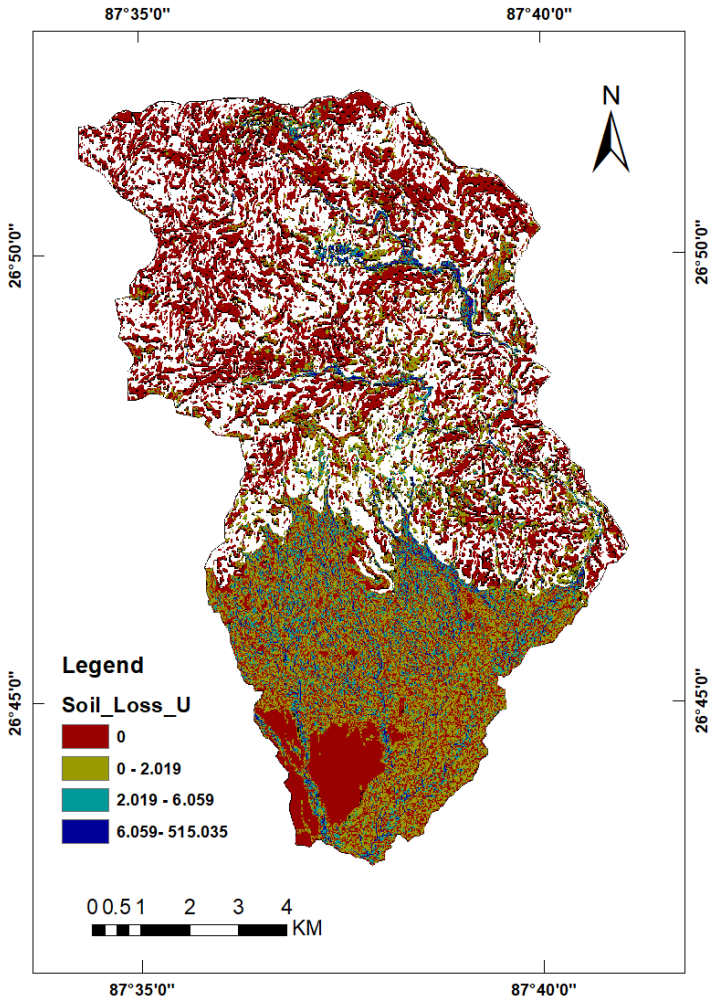

Figure 5.6: Soil Erosion Susceptibility Map Obtained from USLE Model.

The potential soil erosion map of Study Area has been produced in ArcGIS by multiplying the factor maps using RUSLE. It has been found that the erosion ranges from 0 to 5852.88 t ha^{-1} yr^{-1} for the study area.

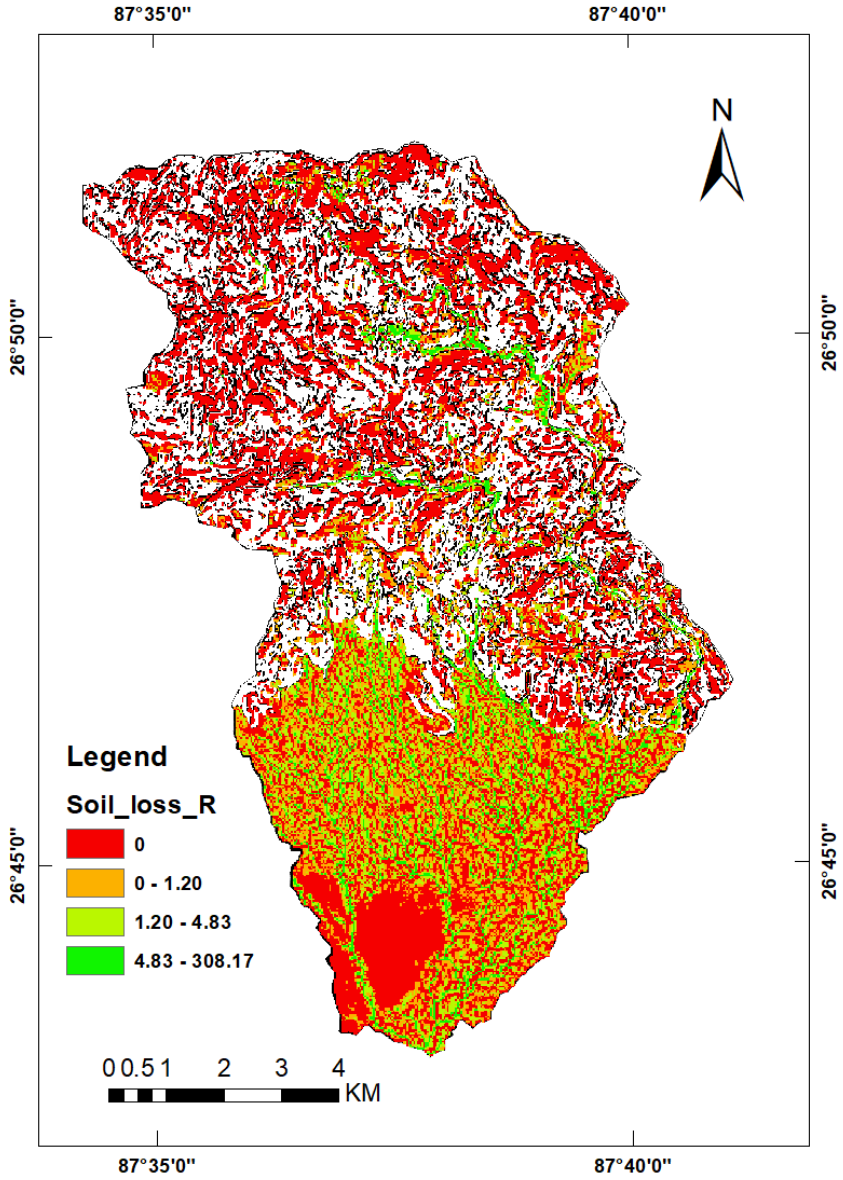

Figure 5.7: Soil Erosion Susceptibility Map Obtained from RUSLE Model.

5.2.1 Soil Erosion Based on Percentage

USLE Method

The result shows that the erosion range from 0 to 515 t ha^{-1} yr^{-1} given by the USLE Method. The maximum erosion was found on the slope with slope percentage ranging from 11.3-17.6 % with minimum on slope ranging from 0-7%.

Table 5.2: Soil Erosion by Slope Obtained from USLE Model.

Slope %	Mean	Min erosion	Maximum
0-7	1.41	0	274.58
7-11.3	2.31	0	389.43
11.3-17.6	3.31	0	515.03
17.6-26.8	1.97	0	404.25
Above 26.8	0.32	0	421.97

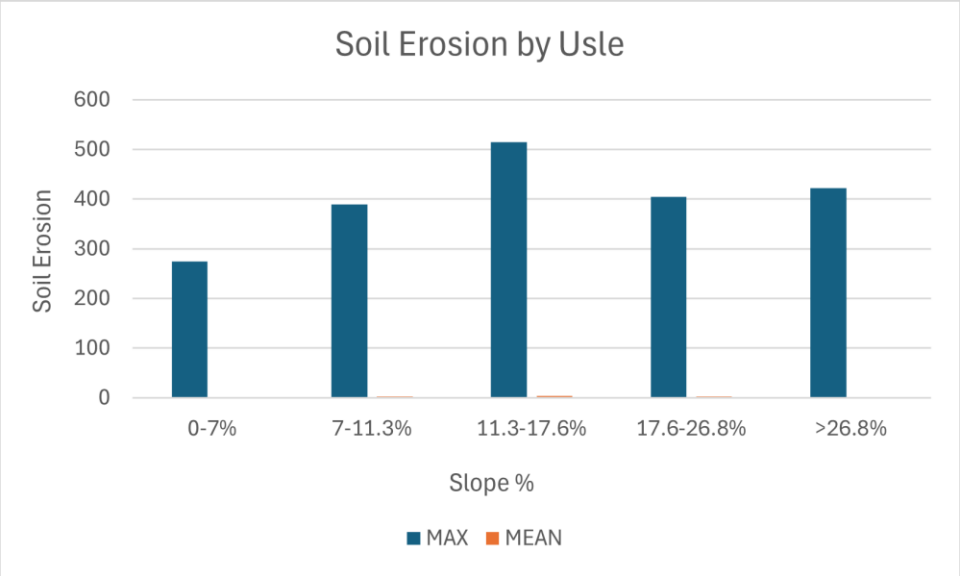

Figure 5.8: Soil Erosion by Slope Obtained from USLE Model.

RUSLE Method

The result shows that the erosion range from 0 to 5852.88 t ha^{-1} yr^{-1} given by the USLE Method. The maximum erosion was found on the slope with slope percentage ranging from above 26.8 % with minimum on slope ranging from 0-7%.

Table 5.3: Soil Erosion by Slope Obtained from RUSLE Model.

Slope %	Mean	Min erosion	Maximum
0-7	**1.71**	**0**	**541.95**
7-11.3	**3.03**	**0**	**490.63**
11.3-17.6	**5.98**	**0**	**928.64**
17.6-26.8	**8.44**	**0**	**2170.75**
Above 26.8	**5.94**	**0**	**5852.88**

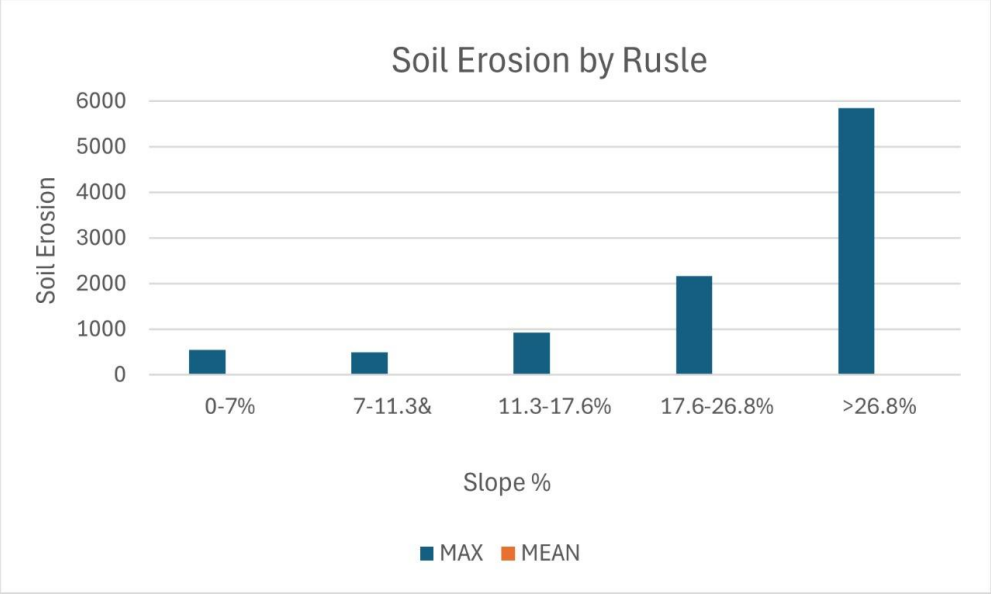

Figure 5.9: Soil Erosion by Slope Obtained from RUSLE Model.

5.2.2 Soil Erosion Based on LULC Classification

USLE Method

The result shows that the erosion range from 0 to 515 t ha^{-1} yr^{-1} given by the USLE Method. The maximum erosion was found on the Riverbed with minimum on forest.

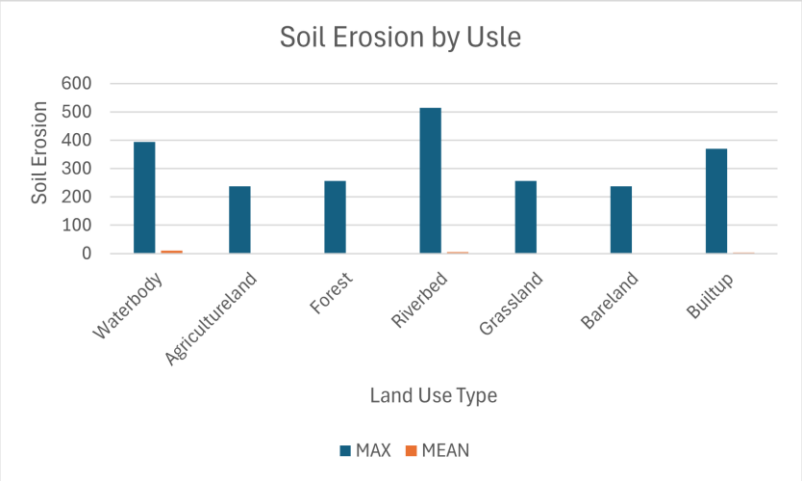

Figure 5.10: Soil Erosion by LULC Obtained from USLE Model.

RUSLE Method

The result shows that the erosion range from 0 to 308 t ha^{-1} yr^{-1} given by the USLE Method. The maximum erosion was found on the Riverbed with minimum on forest.

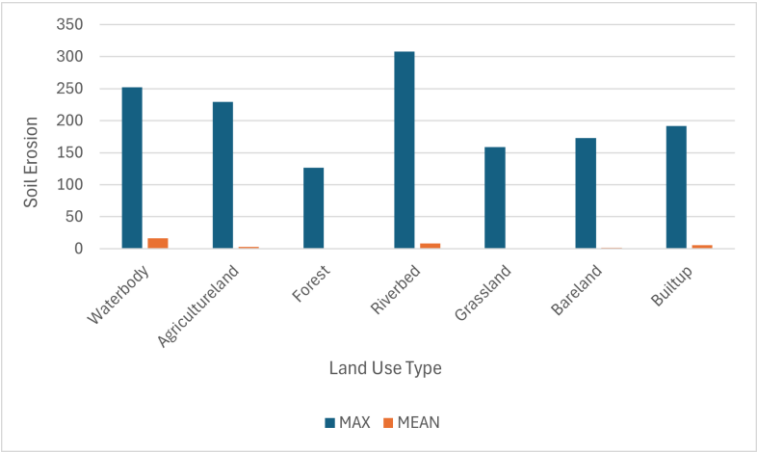

Figure 5.11: Soil Erosion by LULC Obtained from RUSLE Model.

5.3 Model Evaluation, Performance Analysis and validation of susceptibility Map

The erosion susceptibility model of RUSLE and USLE was evaluated separately using the AU-ROC curve, which yielded an AUC value of **0.882 (88%)** and **0.891 (89%)** respectively, indicating high predictive accuracy. Since an AUC closer to 1.0 represents excellent performance and 0.5 suggests random prediction, the result demonstrates that the model effectively distinguishes between erosion-prone and non-erosion areas with a strong balance of sensitivity and specificity, thereby minimizing misclassifications. This high accuracy validates both the selected input factors and the modeling framework, confirming the model's robustness and reliability for identifying erosion hotspots and supporting conservation planning and land management decisions. Fig (5.12) shows the AU-ROC curve of RUSLE and USLE.

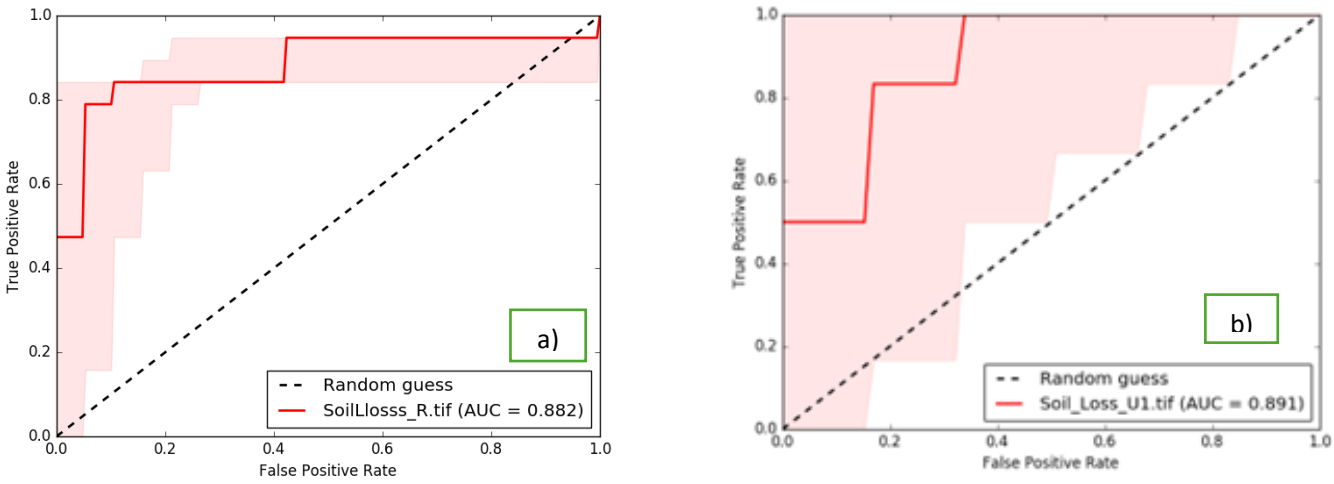

Figure 5.12: Performance Analysis and Validation of Susceptibility Map a) With RUSLE, b) with USLE.

5.4 Result Interpretation and Validation

Result interpretation and validation are critical steps in soil erosion assessment to ensure that model predictions are both scientifically reliable and practically meaningful. Interpretation involves analyzing spatial and temporal patterns of predicted soil loss in relation to key erosion predictors such as rainfall, soil properties, slope, vegetation cover, and land management practices. High erosion values on steep slopes, barren land, or agricultural fields without conservation measures typically confirm the sensitivity of the model to biophysical conditions,

while lower values in forested and well-managed areas highlight the protective role of vegetation and conservation practices. Validation is equally important, as it tests the accuracy of model outputs against independent datasets such as field measurements, sediment yield records, or previously published studies. AU-ROC curve for two models shows strong model evaluation. A strong agreement between observed and predicted values indicates that the model is well-calibrated and suitable for local conditions, whereas discrepancies may suggest the need for input refinement, parameter adjustment, or integration of higher-resolution datasets. Together, interpretation and validation not only enhance the credibility of soil erosion assessments but also support the formulation of evidence-based soil conservation strategies.

Chapter 6: Conclusions

6.1 Conclusions

Soil erosion is a serious problem in mountainous countries such as Nepal, and this is evident in the Bakraha Watershed. The rate of soil erosion in the watershed varies from 0 to 515 t/ha/year with an average rate of 10.51 t/ha/year of USLE model and 0 ton/ha/yr to 5852.88 ton/ha/yr with an average rate of 16.65 ton/ha/yr. The soil erosion risk areas were mapped based on the stakeholders' perceptions. Stakeholders had some knowledge of the physical factors affecting soil erosion (e.g. slope, type of soil, and conservation practices), but they were not aware of the soil erosion effects of contour cultivation. This research provided knowledge to the researchers about soil erosion effects and environmental degradation caused by contour farmland in Bakraha watershed. The participatory GIS map developed in this research, along with other GIS technology, proved valuable to the farmers and researchers for understanding the issues surrounding soil erosion and the possibilities for improved soil conservation management. This study shows that riverbeds, waterbody, and built-up areas need conservation attention to reduce the risk of soil erosion. The mean erosion rate was high in barren lands, followed by agricultural lands, riverbed, grasslands and forests. The highest erosion rates were observed in steep slopes >26.8% from both erosion models. In a country, like Nepal, which lacks continuous and long-term monitoring of erosion hazards, RUSLE erosion modeling to develop a detailed spatial assessment of erosion hazards using remotely sensed data and automated analysis of land cover and slope gradient could be a good option. Followings are the three main conclusions of the study.

- The Bakraha Watershed experiences soil erosion rates ranging from 0–515 t/ha/year (average 10.51 t/ha/year) under the USLE model and 0–5852.88 t/ha/year (average 16.65 t/ha/year) under the RUSLE model.
- Soil erosion in the Bakraha Watershed is severe, especially in barren and agricultural lands, with the highest rates occurring on steep slopes (>26.8%).
- Conservation measures are urgently needed in riverbeds, water bodies, and built-up areas, while advanced GIS and remote sensing tools can support long-term erosion hazard monitoring in Nepal.

6.2 Limitations

Every scientific project has concurrent advantages and disadvantages. This dissertation also has drawbacks associated with the process complexity, uncertainties in predictions, limitations in data quality, and potential misinterpretations which can affect the accuracy of the results and the interpretation of the findings. Following are main drawbacks of this study:

- Focus on sheet and rill erosion only, ignoring gully, bank, and mass-movement process that dominates in steep terrains.
- Errors in rainfall, DEM, soil or Land cover datasets can significantly underestimate erosion results.
- Each raster cell is assumed uniform in slope, soil, and land cover, which oversimplifies natural variability within landscape.

REFERENCES

282. (n.d.). *RAINFALL-EROSION LOSSES FROM CROPLAND EAST OF THE ROCKY MOUNTAINS Guide for Selection of Practices for Soil and Water Conservation AGRICULTURE HANDBOOK NO Cop. 4 CONTENTS*.

Acharya, T. D. (2018). Regional scale landslide hazard assessment using machine learning methods in Nepal. *Esis for: Doctor in EngineeringAdvisor,, Esis for: Doctor in EngineeringAdvisor*.

Alavinia, M., Saleh, F. N., & Asadi, H. (2019). Effects of rainfall patterns on runoff and rainfall-induced erosion. *International Journal of Sediment Research*, *34*(3), 270–278. https://doi.org/https://doi.org/10.1016/j.ijsrc.2018.11.001

Alewell, C., Borrelli, P., Meusburger, K., & Panagos, P. (2019). Using the USLE: Chances, challenges and limitations of soil erosion modelling. In *International Soil and Water Conservation Research* (Vol. 7, Issue 3, pp. 203–225). International Research and Training Center on Erosion and Sedimentation and China Water and Power Press. https://doi.org/10.1016/j.iswcr.2019.05.004

Amare, S., Langendoen, E., Keesstra, S., van der Ploeg, M., Gelagay, H., Lemma, H., & van der Zee, S. E. A. T. M. (2021). Susceptibility to gully erosion: Applying random forest (RF) and frequency ratio (FR) approaches to a small catchment in Ethiopia. *Water (Switzerland)*, *13*(2). https://doi.org/10.3390/w13020216

Aregai, M., & Biedemariam, M. (2019). Human pressure and the abrupt changes on the natural environment: The case of Eritrean refugee settlements in the North western Tigray, Ethiopia. *Journal of Arid Environments*, *166*, 37–42. https://doi.org/https://doi.org/10.1016/j.jaridenv.2019.04.012

Aryal, K. R., Panthi, S., Basukala, R. K., Kharel, R., Gautam, A., Poudel, B., Sharma, S., Adhikari, B., Budha, R. K., Khadka, S., & Pariyar, S. (2023). Soil loss estimation of Karnali river basin, Nepal. *Journal of Sedimentary Environments*, *8*(3), 409–423. https://doi.org/10.1007/s43217-023-00140-y

Avand, M., Mohammadi, M., Mirchooli, F., Kavian, A., & Tiefenbacher, J. P. (2023). A New Approach for Smart Soil Erosion Modeling: Integration of Empirical and Machine-Learning Models. *Environmental Modeling and Assessment*, *28*(1), 145–160. https://doi.org/10.1007/s10666-022-09858-x

Ávila, F. F., Alvalá, R. C., Mendes, R. M., & Amore, D. J. (2021). The influence of land use/land cover variability and rainfall intensity in triggering landslides: a back-analysis study via physically based models. *Natural Hazards*, *105*(1), 1139–1161. https://doi.org/10.1007/s11069-020-04324-x

Babu, R. (1978). *Determination of erosion index and isoerodent map of India*.

Balabathina, V. N., Raju, R. P., Mulualem, W., & Tadele, G. (2020). Estimation of soil loss using remote sensing and GIS-based universal soil loss equation in northern catchment of Lake Tana Sub-basin, Upper Blue Nile Basin, Northwest Ethiopia. *Environmental Systems Research*, *9*(1), 35. https://doi.org/10.1186/s40068-020-00203-3

Bastola, S., Jeong Seong, Y., Hyup Lee, S., & Shin, Y. (2019). Assessment of Soil Erosion Loss by Using RUSLE and GIS in the Bagmati Basin of Nepal. *Journal of the Korean Geo-Environmental Society*, *20*(3), 5–14.

Bhandari, K. P., Aryal, J., & Darnsawasdi, R. (2015). A geospatial approach to assessing soil erosion in a watershed by integrating socio-economic determinants and the RUSLE model. *Natural Hazards*, *75*(1), 321–342. https://doi.org/10.1007/s11069-014-1321-2

Bhat, S. A., Dar, M. U. D., & Meena, R. S. (2019). *Soil Erosion and Management Strategies BT - Sustainable Management of Soil and Environment* (R. S. Meena, S. Kumar, J. S. Bohra, & M. L. Jat, Eds.; pp. 73–122). Springer Singapore. https://doi.org/10.1007/978-981-13-8832-3_3

Bollati, I. M., Masseroli, A., Mortara, G., Pelfini, M., & Trombino, L. (2019). Alpine gullies system evolution: erosion drivers and control factors. Two examples from the western Italian Alps. *Geomorphology*, *327*, 248–263. https://doi.org/https://doi.org/10.1016/j.geomorph.2018.10.025

Borrelli, P., Alewell, C., Alvarez, P., Anache, J. A. A., Baartman, J., Ballabio, C., Bezak, N., Biddoccu, M., Cerdà, A., Chalise, D., Chen, S., Chen, W., De Girolamo, A. M., Gessesse, G. D., Deumlich, D., Diodato, N., Efthimiou, N., Erpul, G., Fiener, P., … Panagos, P. (2021). Soil erosion modelling: A global review and statistical analysis. *Science of the Total Environment*, *780*. https://doi.org/10.1016/j.scitotenv.2021.146494

Chalise, D., Kumar, L., & Kristiansen, P. (2019). Land degradation by soil erosion in Nepal: A review. In *Soil Systems* (Vol. 3, Issue 1, pp. 1–18). MDPI AG. https://doi.org/10.3390/soilsystems3010012

Chen, Z., Liang, S., Ke, Y., Yang, Z., & Zhao, H. (2019). Landslide susceptibility assessment using evidential belief function, certainty factor and frequency ratio model at Baxie River basin, NW China. *Geocarto International*, *34*(4), 348–367. https://doi.org/10.1080/10106049.2017.1404143

Dahal, R. (2020). Soil Erosion Estimation Using RUSLE Modeling and Geospatial Tool: Case Study of Kathmandu District, Nepal. *Forestry: Journal of Institute of Forestry, Nepal*, *17*(17), 118–134. https://doi.org/10.3126/forestry.v17i0.33627

Dijkshoorn, K., & Huting, J. (2009). *Soil and Terrain database for Nepal (1:1 million) Front cover: Soils of the SOTER map for Nepal SOTER database for Nepal*.

DK Mccool, & LC Brown. (1987). *Revised slope steepness factor for the Universal Soil Loss Equation*.

Du, X., Jian, J., Du, C., & Stewart, R. D. (2022). Conservation management decreases surface runoff and soil erosion. *International Soil and Water Conservation Research*, *10*(2), 188–196. https://doi.org/https://doi.org/10.1016/j.iswcr.2021.08.001

Dunkerley, D. (2021). Rainfall drop arrival rate at the ground: A potentially informative parameter in the experimental study of infiltration, soil erosion, and related land surface processes. *CATENA*, *206*, 105552. https://doi.org/https://doi.org/10.1016/j.catena.2021.105552

Eekhout, J. P. C., & de Vente, J. (2022). Global impact of climate change on soil erosion and potential for adaptation through soil conservation. *Earth-Science Reviews*, *226*, 103921. https://doi.org/https://doi.org/10.1016/j.earscirev.2022.103921

Epple, L., Kaiser, A., Schindewolf, M., Bienert, A., Lenz, J., & Eltner, A. (2022). A Review on the Possibilities and Challenges of Today's Soil and Soil Surface Assessment Techniques in the Context of Process-Based Soil Erosion Models. *Remote Sensing*, *14*(10). https://doi.org/10.3390/rs14102468

Fan, Y., Clark, M., Lawrence, D. M., Swenson, S., Band, L. E., Brantley, S. L., Brooks, P. D., Dietrich, W. E., Flores, A., Grant, G., Kirchner, J. W., Mackay, D. S., McDonnell, J. J., Milly, P. C. D., Sullivan, P. L., Tague, C., Ajami, H., Chaney, N., Hartmann, A., … Yamazaki, D. (2019). Hillslope Hydrology in Global Change Research and Earth System Modeling. *Water Resources Research*, *55*(2), 1737–1772. https://doi.org/https://doi.org/10.1029/2018WR023903

FAO, F. A. agriculture organization of T. U. N. (2021). *Systems at breaking point*. http://www.fao.org/3/cb7654en/cb7654en.pdf

Fernández, D., Adermann, E., Pizzolato, M., Pechenkin, R., Rodríguez, C. G., & Taravat, A. (2023). Comparative Analysis of Machine Learning Algorithms for Soil Erosion Modelling Based on Remotely Sensed Data. *Remote Sensing*, *15*(2), 1–20. https://doi.org/10.3390/rs15020482

Firoozi, A. A., & Firoozi, A. A. (2024). Water erosion processes: Mechanisms, impact, and management strategies. *Results in Engineering*, *24*. https://doi.org/10.1016/j.rineng.2024.103237

Fu, B., Merritt, W. S., Croke, B. F. W., Weber, T. R., & Jakeman, A. J. (2019). A review of catchment-scale water quality and erosion models and a synthesis of future prospects. *Environmental Modelling & Software*, *114*, 75–97. https://doi.org/https://doi.org/10.1016/j.envsoft.2018.12.008

Ghimire, M. (2020). *Basin characteristics, river morphology, and process in the Chure-Terai landscape: A case study of the Bakraha river, East Nepal*. *13*, 107–142.

Ghimire, S. K., Higaki, D., & Bhattarai, T. P. (2013a). Estimation of soil erosion rates and eroded sediment in a degraded catchment of the Siwalik Hills, Nepal. *Land*, *2*(3), 370–391. https://doi.org/10.3390/land2030370

Ghimire, S. K., Higaki, D., & Bhattarai, T. P. (2013b). Estimation of soil erosion rates and eroded sediment in a degraded catchment of the Siwalik Hills, Nepal. *Land*, *2*(3), 370–391. https://doi.org/10.3390/land2030370

Giupponi, L., Borgonovo, G., Giorgi, A., & Bischetti, G. B. (2019). How to renew soil bioengineering for slope stabilization: some proposals. *Landscape and Ecological Engineering*, *15*(1), 37–50. https://doi.org/10.1007/s11355-018-0359-9

Greco, R., Marino, P., & Bogaard, T. A. (2023). Recent advancements of landslide hydrology. *WIREs Water*, *10*(6), e1675. https://doi.org/https://doi.org/10.1002/wat2.1675

Guzzetti, F., Gariano, S. L., Peruccacci, S., Brunetti, M. T., & Melillo, M. (2022). *Chapter 15 - Rainfall and landslide initiation* (R. B. T.-R. Morbidelli, Ed.; pp. 427–450). Elsevier. https://doi.org/https://doi.org/10.1016/B978-0-12-822544-8.00012-3

Haruna, S. I., Anderson, S. H., Udawatta, R. P., Gantzer, C. J., Phillips, N. C., Cui, S., & Gao, Y. (2020). Improving soil physical properties through the use of cover crops: A review. *Agrosystems, Geosciences & Environment*, *3*(1), e20105. https://doi.org/https://doi.org/10.1002/agg2.20105

Highland, L. M., & Bobrowsky, P. (2008). The landslide Handbook - A guide to understanding landslides. *US Geological Survey Circular*, *1325*, 1–147.

Joshi, P., Adhikari, R., Bhandari, R., Shrestha, B., Shrestha, N., Chhetri, S., Sharma, S., & Routh, J. (2023). Himalayan watersheds in Nepal record high soil erosion rates estimated using the RUSLE model and experimental erosion plots. *Heliyon*, *9*(5), e15800. https://doi.org/10.1016/j.heliyon.2023.e15800

Khanal, B. R., Lamichhane, S., Sharma Acharya, B., Tiruwa, D. B., Bahadur, D., Babu, T., & Khanal, R. (2021). Soil erosion estimation using Geographic Information System (GIS) and Revised Universal Soil Loss Equation (RUSLE) in the Siwalik Hills of Nawalparasi, Nepal Corrected Proof Soil erosion estimation using Geographic Information System

(GIS) and Revised Universal Soil Loss Equation (RUSLE) in the Siwalik Hills of Nawalparasi, Nepal. *Article in Journal of Water and Climate Change*. https://doi.org/10.2166/wcc

Koirala, P., Thakuri, S., Joshi, S., & Chauhan, R. (2019). Estimation of Soil Erosion in Nepal using a RUSLE modeling and geospatial tool. *Geosciences (Switzerland)*, *9*(4). https://doi.org/10.3390/geosciences9040147

Lal, R. (2006). *Influence of soil erosion on carbon dynamics in the world*.

Li, P., Chen, J., Zhao, G., Holden, J., Liu, B., Chan, F. K. S., Hu, J., Wu, P., & Mu, X. (2022). Determining the drivers and rates of soil erosion on the Loess Plateau since 1901. *Science of The Total Environment*, *823*, 153674. https://doi.org/https://doi.org/10.1016/j.scitotenv.2022.153674

Luo, Y., Zhao, X., Li, Y., Liu, X., Wang, L., Wang, X., & Du, Z. (2021). Wind disturbance on litter production affects soil carbon accumulation in degraded sandy grasslands in semi-arid sandy grassland. *Ecological Engineering*, *171*, 106373. https://doi.org/https://doi.org/10.1016/j.ecoleng.2021.106373

Mandal, U. K., & Kumari, K. (2020). Geospatial technology based soil loss estimation for sustainable urban development of butwal Submetropolitan City, Nepal. *International Archives of the Photogrammetry, Remote Sensing and Spatial Information Sciences - ISPRS Archives*, *43*(B3), 137–144. https://doi.org/10.5194/isprs-archives-XLIII-B3-2020-137-2020

McAdoo, B. G., Quak, M., Gnyawali, K. R., Adhikari, B. R., Devkota, S., Lal Rajbhandari, P., & Sudmeier-Rieux, K. (2018). Roads and landslides in Nepal: How development affects environmental risk. *Natural Hazards and Earth System Sciences*, *18*(12), 3203–3210. https://doi.org/10.5194/nhess-18-3203-2018

Medina, V., Hürlimann, M., Guo, Z., Lloret, A., & Vaunat, J. (2021). Fast physically-based model for rainfall-induced landslide susceptibility assessment at regional scale. *CATENA*, *201*, 105213. https://doi.org/https://doi.org/10.1016/j.catena.2021.105213

Negese, A. (2021). Impacts of Land Use and Land Cover Change on Soil Erosion and Hydrological Responses in Ethiopia. *Applied and Environmental Soil Science*, *2021*(1), 6669438. https://doi.org/https://doi.org/10.1155/2021/6669438

Okamura, M., Bhandary, N. P., Mori, S., Marasini, N., & Hazarika, H. (2015). Report on a reconnaissance survey of damage in Kathmandu caused by the 2015 Gorkha Nepal earthquake. *Soils and Foundations*, *55*(5), 1015–1029. https://doi.org/10.1016/j.sandf.2015.09.005

Onet, A., Dincă, L. C., Grenni, P., Laslo, V., Teusdea, A. C., Vasile, D. L., Enescu, R. E., & Crisan, V. E. (2019). Biological indicators for evaluating soil quality improvement in a soil degraded by erosion processes. *Journal of Soils and Sediments*, *19*(5), 2393–2404. https://doi.org/10.1007/s11368-018-02236-9

Owens, P. N. (2020). Soil erosion and sediment dynamics in the Anthropocene: a review of human impacts during a period of rapid global environmental change. *Journal of Soils and Sediments*, *20*(12), 4115–4143. https://doi.org/10.1007/s11368-020-02815-9

Pimentel, D. (2006). Soil erosion: A food and environmental threat. *Environment, Development and Sustainability*, *8*(1), 119–137. https://doi.org/10.1007/s10668-005-1262-8

Prancevic, J. P., & Kirchner, J. W. (2019). Topographic Controls on the Extension and Retraction of Flowing Streams. *Geophysical Research Letters*, *46*(4), 2084–2092. https://doi.org/https://doi.org/10.1029/2018GL081799

Pulley, S., & Collins, A. L. (2024). Soil erosion, sediment sources, connectivity and suspended sediment yields in UK temperate agricultural catchments: Discrepancies and reconciliation of field-based measurements. *Journal of Environmental Management*, *351*, 119810. https://doi.org/https://doi.org/10.1016/j.jenvman.2023.119810

Raimondi, L., Pepe, G., Firpo, M., Calcaterra, D., & Cevasco, A. (2023). An open-source and QGIS-integrated physically based model for Spatial Prediction of Rainfall-Induced Shallow Landslides (SPRIn-SL). *Environmental Modelling & Software*, *160*, 105587. https://doi.org/https://doi.org/10.1016/j.envsoft.2022.105587

Raya, B. (2023). Soil erosion and environmental degradation in Nepal: A Review of Environmental Policies. *The Third Pole: Journal of Geography Education*, *23*, 15–29.

Regmi, A. D., Yoshida, K., Pourghasemi, H. R., DhitaL, M. R., & Pradhan, B. (2014). Landslide susceptibility mapping along Bhalubang — Shiwapur area of mid-Western Nepal using frequency ratio and conditional probability models. *Journal of Mountain Science*, *11*(5), 1266–1285. https://doi.org/10.1007/s11629-013-2847-6

Renard *'a, K. G., & Freimund, J. R. (1994). Using monthly precipitation data to estimate the R-factor in the revised USLE. In *Journal of Hydrology ELSEVIER* (Vol. 1).

Rivera, A., Bravo, C., & Buob, G. (2017). Climate Change and Land Ice. *International Encyclopedia of Geography*, 1–15. https://doi.org/10.1002/9781118786352.wbieg0538

Sene, K. (2024). *Hydrological Forecasting BT - Hydrometeorology: Forecasting and Applications* (K. Sene, Ed.; pp. 167–215). Springer Nature Switzerland. https://doi.org/10.1007/978-3-031-58269-1_5

Siwakoti, D. R. (2000). An assessment of soil loss and natural hazards in Nepal. *Journal of Nepal Geological Society*, *21*, 41–48.

Smith, P., Calvin, K., Nkem, J., Campbell, D., Cherubini, F., Grassi, G., Korotkov, V., Le Hoang, A., Lwasa, S., McElwee, P., Nkonya, E., Saigusa, N., Soussana, J. F., Taboada, M. A., Manning, F. C., Nampanzira, D., Arias-Navarro, C., Vizzarri, M., House, J., … Arneth, A. (2020). Which practices co-deliver food security, climate change mitigation and adaptation, and combat land degradation and desertification? *Global Change Biology*, *26*(3), 1532–1575. https://doi.org/10.1111/gcb.14878

Spiekermann, R. I., Smith, H. G., McColl, S., Burkitt, L., & Fuller, I. C. (2022). Development of a morphometric connectivity model to mitigate sediment derived from storm-driven shallow landslides. *Ecological Engineering*, *180*, 106676. https://doi.org/https://doi.org/10.1016/j.ecoleng.2022.106676

Stephens, C. M., Lall, U., Johnson, F. M., & Marshall, L. A. (2021). Landscape changes and their hydrologic effects: Interactions and feedbacks across scales. *Earth-Science Reviews*, *212*, 103466. https://doi.org/https://doi.org/10.1016/j.earscirev.2020.103466

Tiruwa, D. B., Khanal, B. R., Lamichhane, S., & Acharya, B. S. (2021a). Soil erosion estimation using geographic information system (Gis) and revised universal soil loss equation (rusle) in the siwalik hills of nawalparasi, nepal. *Journal of Water and Climate Change*, *12*(5), 1958–1974. https://doi.org/10.2166/wcc.2021.198

Tiruwa, D. B., Khanal, B. R., Lamichhane, S., & Acharya, B. S. (2021b). Soil erosion estimation using geographic information system (Gis) and revised universal soil loss equation (rusle) in the siwalik hills of nawalparasi, nepal. *Journal of Water and Climate Change*, *12*(5), 1958–1974. https://doi.org/10.2166/wcc.2021.198

Urbina, C. A. F., van Dam, J. C., Hendriks, R. F. A., van den Berg, F., Gooren, H. P. A., & Ritsema, C. J. (2019). Water Flow in Soils with Heterogeneous Macropore Geometries. *Vadose Zone Journal*, *18*(1), 190015. https://doi.org/https://doi.org/10.2136/vzj2019.02.0015

van Leeuwen, C. C. E., Cammeraat, E. L. H., de Vente, J., & Boix-Fayos, C. (2019). The evolution of soil conservation policies targeting land abandonment and soil erosion in Spain: A review. *Land Use Policy*, *83*, 174–186. https://doi.org/https://doi.org/10.1016/j.landusepol.2019.01.018

Wang, C., Fu, X., Zhang, X., Wang, X., Zhang, G., & Gong, Z. (2024). Modeling soil erosion dynamic processes along hillslopes with vegetation impact across different land uses on the Loess Plateau of China. *CATENA*, *243*, 108202. https://doi.org/https://doi.org/10.1016/j.catena.2024.108202

Webster, R. (2005). Morgan, R.P.C. Soil Erosion and Conservation, 3rd edition. Blackwell Publishing, Oxford, 2005. x + 304 pp. £29.95, paperback. ISBN 1-4051-1781-8. *European Journal of Soil Science - EUR J SOIL SCI*, *56*, 686. https://doi.org/10.1111/j.1365-2389.2005.0756f.x

WH Wischmeier, & DD Smith. (1978). *Predicting rainfall erosion losses: a guide to conservation planning*.

Wilkes, M. A., Gittins, J. R., Mathers, K. L., Mason, R., Casas-Mulet, R., Vanzo, D., Mckenzie, M., Murray-Bligh, J., England, J., Gurnell, A., & Jones, J. I. (2019). Physical and

biological controls on fine sediment transport and storage in rivers. *WIREs Water*, *6*(2), e1331. https://doi.org/https://doi.org/10.1002/wat2.1331

Wu, B., Wang, Z., Zhang, Q., Shen, N., & Liu, J. (2019). Evaluating and modelling splash detachment capacity based on laboratory experiments. *CATENA*, *176*, 189–196. https://doi.org/https://doi.org/10.1016/j.catena.2019.01.009

Yuan, L., Zhang, X.-C. (John), Busteed, P., Flanagan, D. C., & Srivastava, A. (2022). Modeling surface runoff and soil loss response to climate change under GCM ensembles and multiple cropping and tillage systems in Oklahoma. *Soil and Tillage Research*, *218*, 105296. https://doi.org/https://doi.org/10.1016/j.still.2021.105296

Zhang, Y., Degroote, J., Wolter, C., & Sugumaran, R. (2009). Integration of modified universal soil loss equation (Musle) into a GIS framework to assess soil erosion risk. *Land Degradation and Development*, *20*(1), 84–91. https://doi.org/10.1002/ldr.893

Zhu, H., & Zhang, L. (2019). Root-soil-water hydrological interaction and its impact on slope stability. *Georisk: Assessment and Management of Risk for Engineered Systems and Geohazards*, *13*(4), 349–359. https://doi.org/10.1080/17499518.2019.1616098

APPENDICES

Appendix A: Results of Sieve Analysis and Hydrometer Testing

Appendix B: Field Visit and Survey Photographs

Appendix C: Sample Collection Photographs

Appendix D: Coordinates of Sampling Hotspots

Appendix E: Laboratory Testing Photographs

Appendix F: Soil Properties Data

Appendix A: Results of Sieve Analysis and Hydrometer Testing

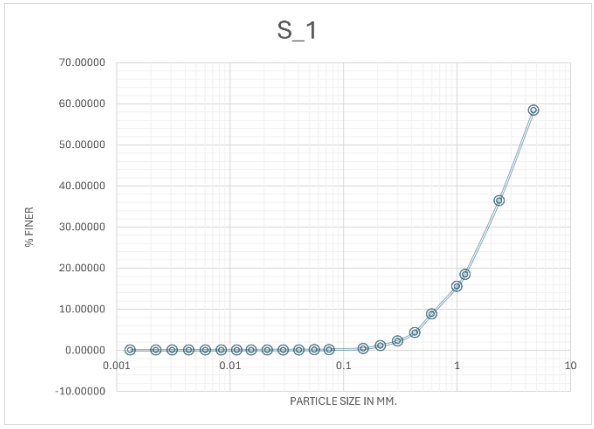

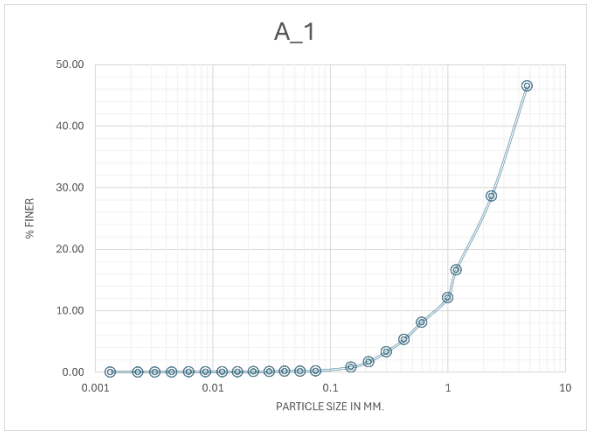

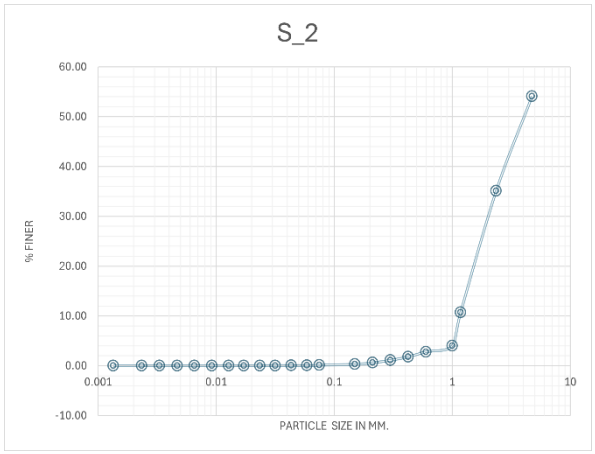

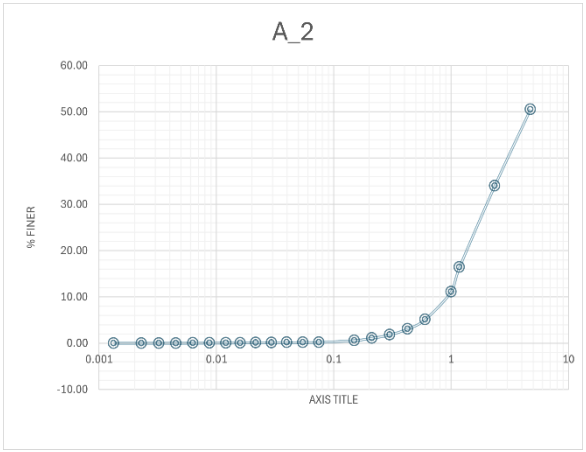

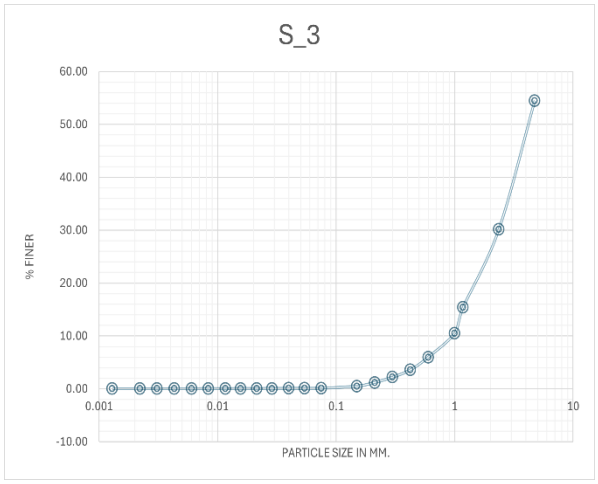

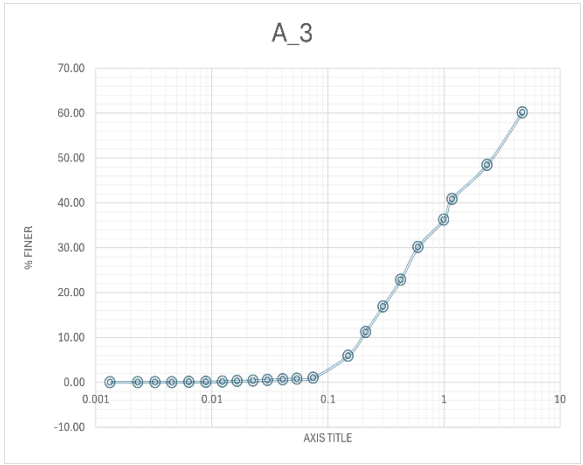

Figure A1: Gradation Curve and Particle Size Distribution analysis

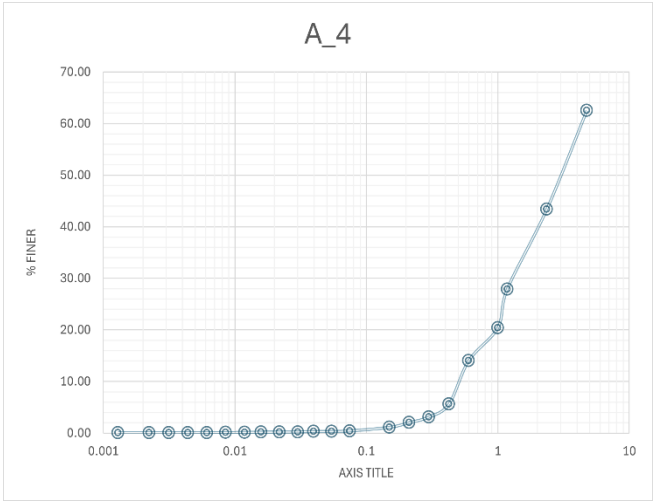

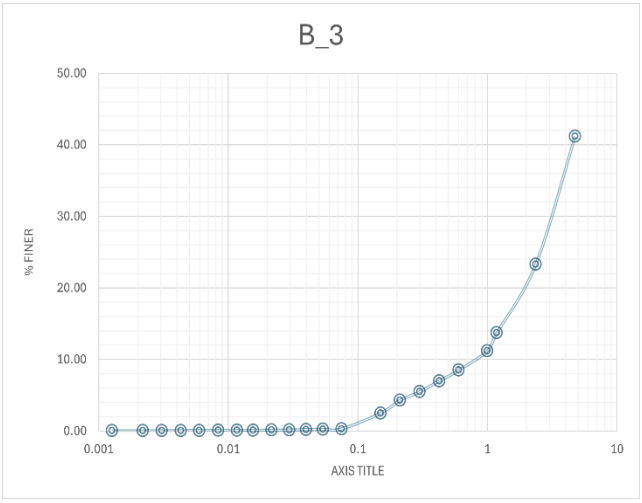

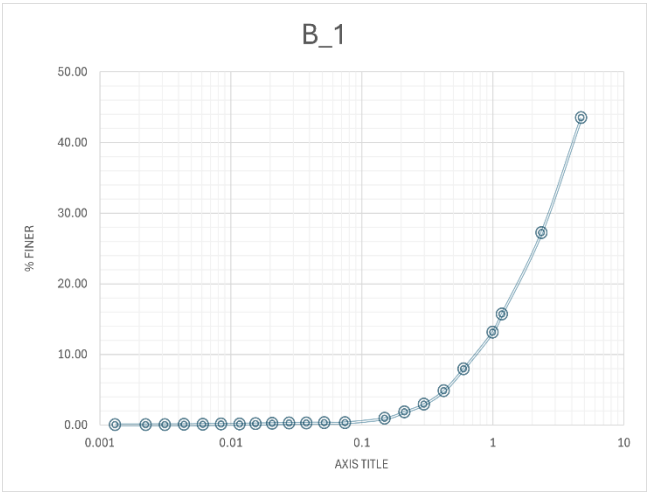

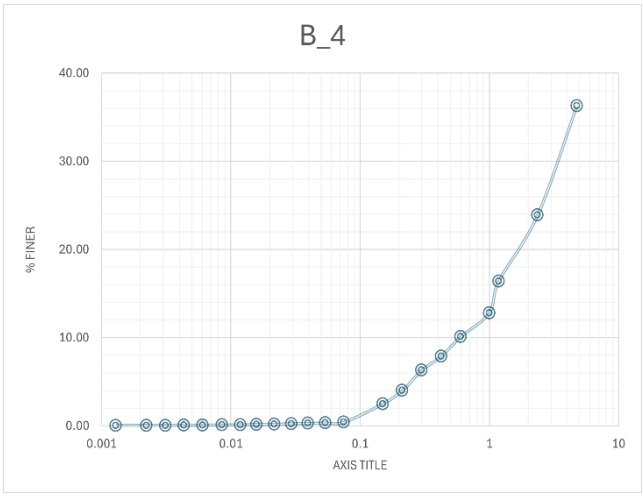

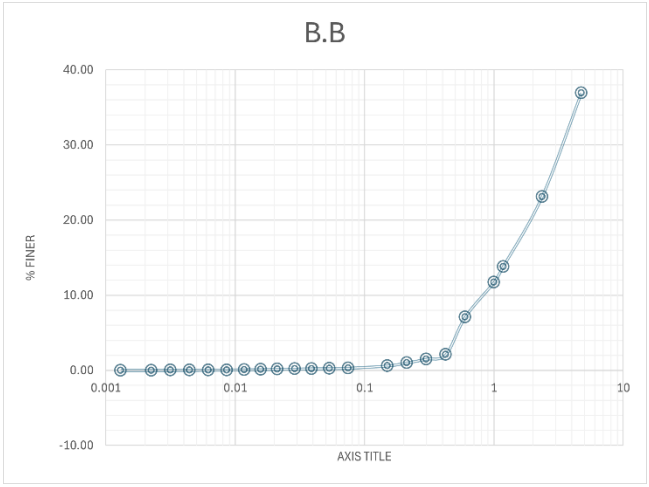

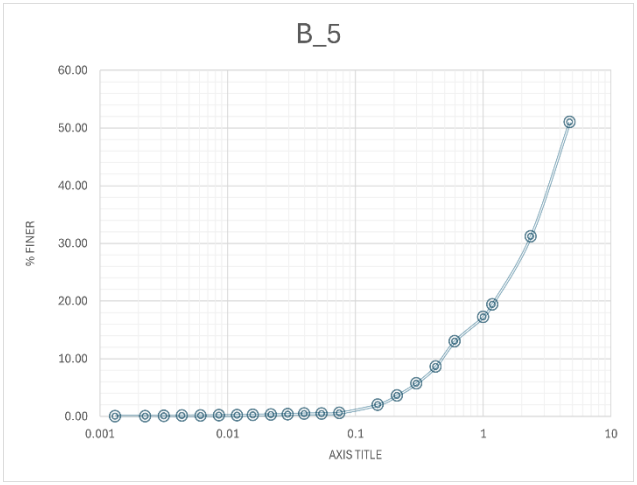

Figure A2: Gradation Curve and Particle Size Distribution analysis

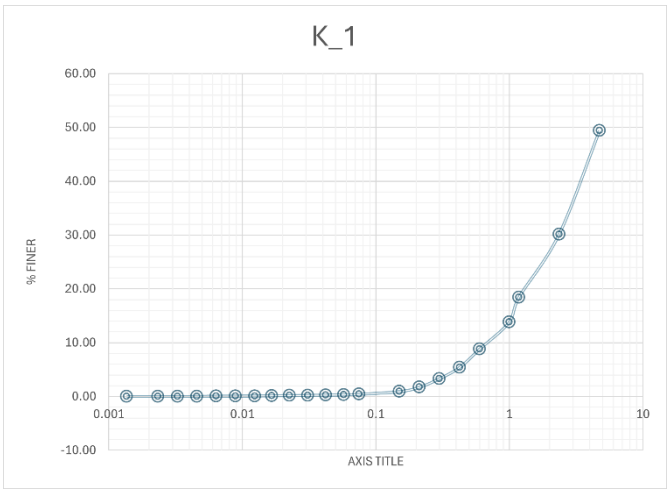

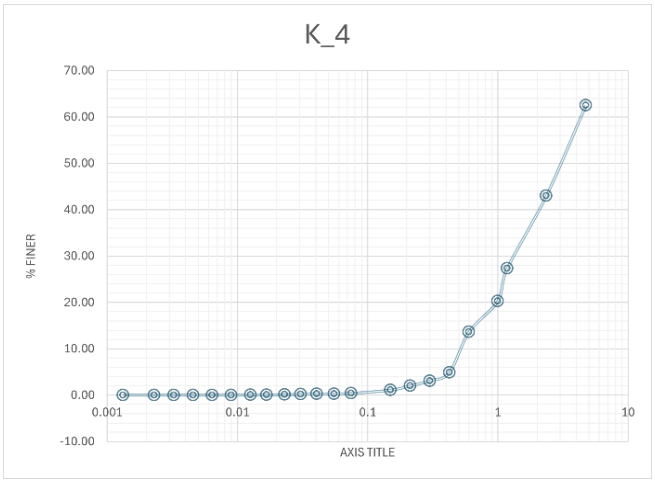

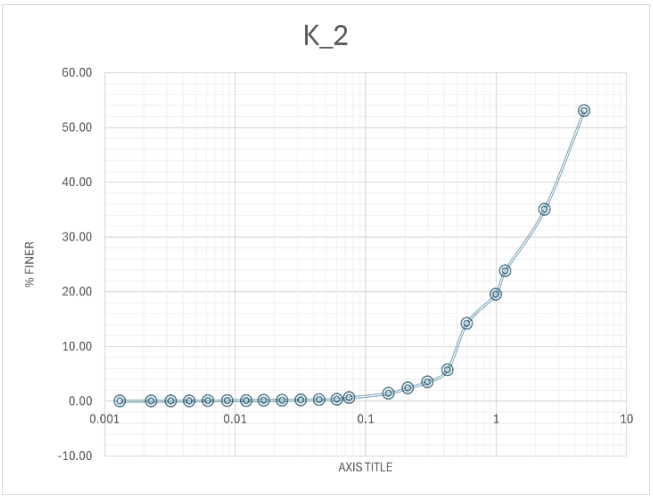

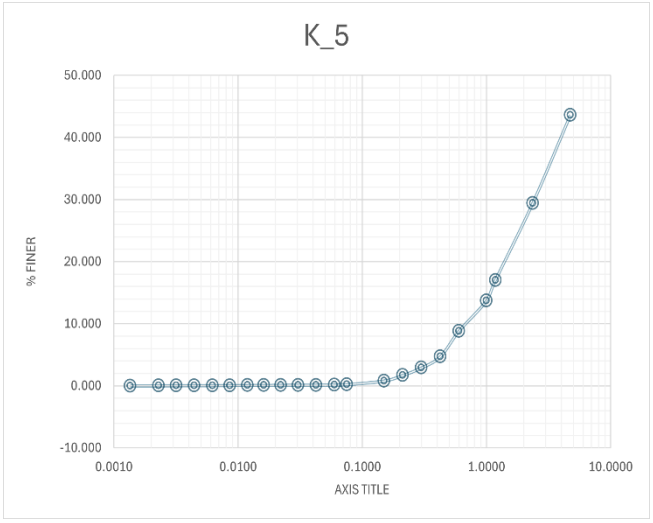

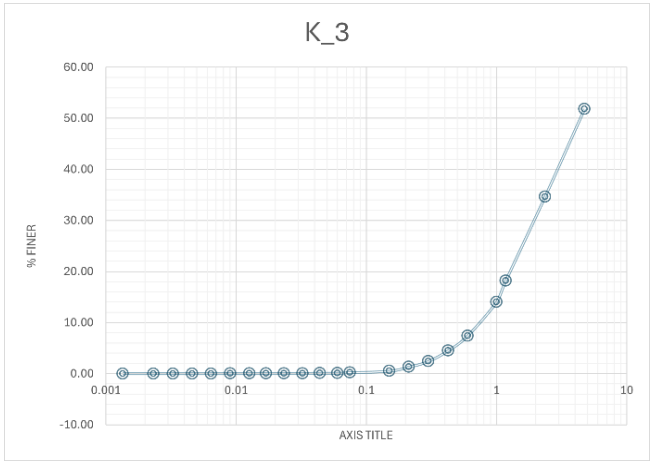

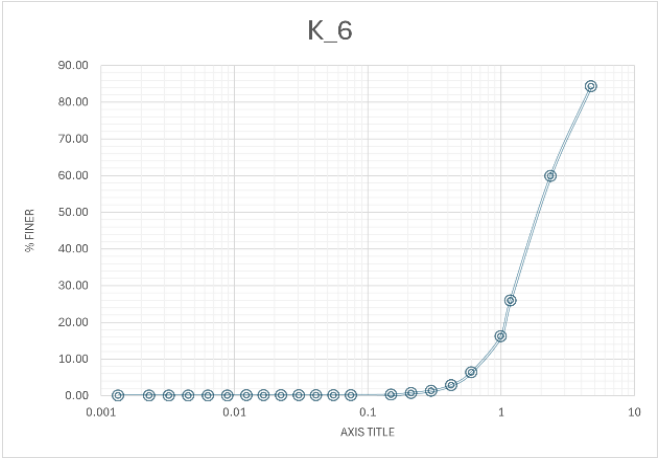

Figure A3: Gradation Curve and Particle Size Distribution analysis

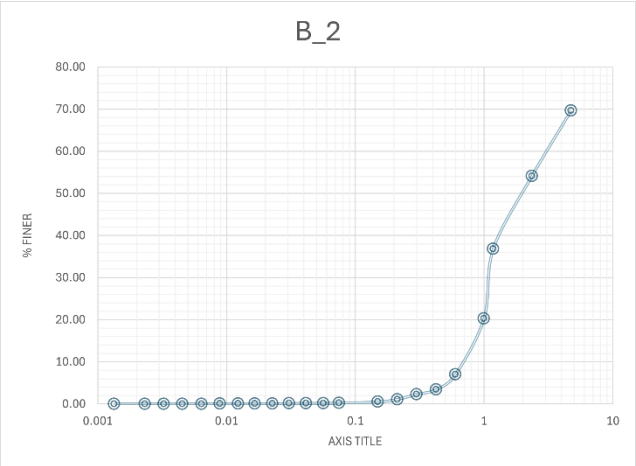

Figure A4: Gradation Curve and Particle Size Distribution analysis

Appendix B: Field Visit and Survey Photographs

Figure B1: Photographs Showing the Existing Soil Hotspots within Study Area

Figure B2: Photographs Showing the Existing Soil Hotspots within Study Area

Appendix C: Sample Collection Photographs

Figure C1: Collecting Soil Samples from Various Existing Soil Erosion Location

Appendix D: Coordinates of Sampling Hotspots

Table D.1: Coordinates of Identified Erosion Hotspots

SN	Designation of Erosion Hotspots	Coordinates	
		Latitude	Longitude
1	A_1	26°48'4.49"N	87°37'36.31"E
2	A_2	26°47'49.62"N	87°38'6.82"E
3	A_3	26°47'38.60"N	87°38'43.85"E
4	A_4	26°47'28.18"N	87°37'46.19"E
5	B.B	26°49'3.56"N	87°35'23.45"E
6	B_1	26°47'24.29"N	87°38'21.80"E
7	B_2	26°47'26.39"N	87°38'28.84"E
8	B_3	26°47'29.62"N	87°38'22.22"E
9	B_4	26°46'41.51"N	87°38'40.25"E
10	B_5	26°46'47.80"N	87°38'28.24"E
11	K_1	26°47'11.36"N	87°40'29.87"E
12	K_2	26°47'48.65"N	87°39'25.53"E
13	K_3	26°49'56.63"N	87°37'43.94"E
14	K_4	26°48'53.67"N	87°39'43.41"E
15	K_5	26°46'58.45"N	87°39'26.96"E
16	K_6	26°46'22.58"N	87°39'44.67"E
17	S_1	26°48'44.46"N	87°37'10.30"E
18	S_2	26°48'33.82"N	87°36'26.78"E
19	S_3	26°48'22.94"N	87°36'54.96"E

Appendix E: Laboratory Testing Photographs

Figure E1: Photograph Showing Hydrometer Testing in Laboratory

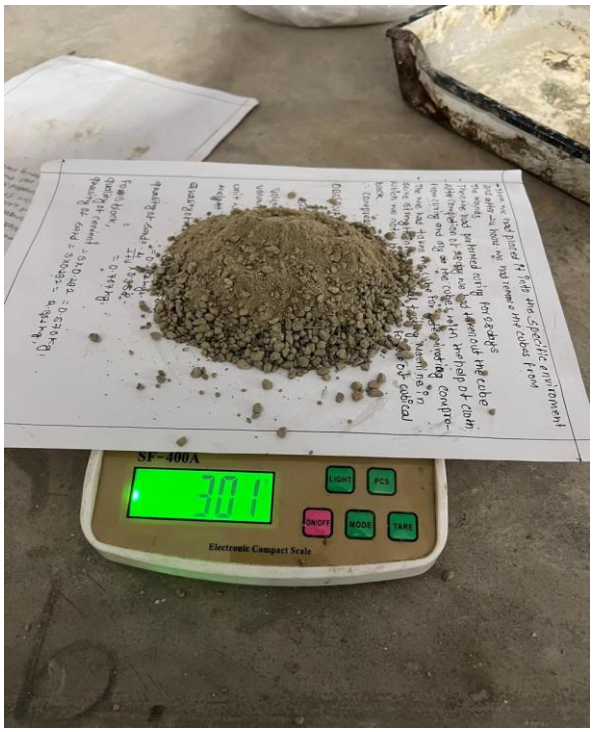

Figure E2: Photograph Showing Pycnometer Test and Sieve Analysis Laboratory